

How 5G is making us rethink UE antenna design

White paper



Contents

Introduction	3
mmWave inclusion in 5G NR	4
3GPP mmWave vision	6
3GPP radiated performance requirements	7
5G NR device mmWave antenna implementation	9
Implementation in a smart phone	9
Typical smart phone antenna performance	11
Free space radiation patterns	12
Right-hand browsing grip radiation patterns	15
Dual-hand browsing grip radiation patterns	18
Dual-hand gamer grip radiation patterns	21
Radiated efficiency	24
Max peak EIRP and spherical coverage	25
3GPP antenna and blocking models	26
User interaction comparison with FR1 implementation	33
XR antenna implementation for 5G NR	33
3GPP requirements	35
Envisioned implementation on a pair of glasses and expected performance	36
Alternative implementation on a pair of glasses and expected performance	41
Estimated performance for an mmWave antenna array on a pair of XR reference glasses	44
Alternative mmWave antenna solution	47
Conclusion	49
Abbreviations	50
References	51



Introduction

Cellular wireless communication has been an enormously successful technology ever since the first generation of commercial systems emerged in the 1980s from companies like Nordic Mobile Telephone (NMT) and American Mobile Phone System (AMPS). The devices for these systems were big, expensive, and could only be used for voice communication. They were also very heavy, which meant they were typically only suitable for installing in vehicles. However, each new generation of cellular wireless communication has reduced the size, weight and cost of the devices, which has dramatically increased the number of subscribers using them. Each new generation has also introduced new features, the most significant of which is data transfer. Starting with the simple Short Message Service (SMS), data transfer capabilities have evolved to include the full-blown browsing capabilities seen on most handheld devices today. These capabilities require cellular networks to support very high data rates.

This success continues to challenge the capacity of cellular networks. As a result, each new generation of the 3rd Generation Partnership Project (3GPP) cellular wireless communication standards has introduced new usable frequency bands to increase connectivity around the world, as well as new Carrier Aggregation (CA) combinations, driven by operators, to improve scheduling flexibility, maximize network efficiency, throughput and coverage. These features require the device to support a higher number of frequency ranges, a larger total frequency span, and an increased number of simultaneously active bands, which increases the complexity of the antenna design and its implementation into the form factor of the device.

The primary frequency range for 3GPP goes from 410 MHz to 7125 MHz and is referred to as Frequency Range 1 (FR1). FR1 is broken down into the following bands:

- Low-Band (LB): below 960 MHz
- Mid-Low-Band (MLB): from 1427 MHz to 1518 MHz
- Mid-Band (MB): from 1710 MHz to 2170 MHz
- High-Band (HB): from 2200 MHz to 2690 MHz
- Ultra-High-Band (UHB): from 3300 MHz to 7125 MHz

High-end cellular devices typically support Multiple Input Multiple Output (MiMo), a wireless technology that uses multiple transmitters and receivers to transfer more data at the same time. These devices support 2x2 MiMo for LB and 4x4 MiMo for MLB, MB, HB and UHB.

Cellular devices must have a minimum of four antennas integrated into the form factor to support MiMo technology. However, many devices are implemented with more than one antenna to cover the relatively large frequency span from LB to UHB, and the actual number of antennas implemented to support MiMo for FR1 can easily be more than 10.

One of the new additions in the fifth generation of cellular wireless communications (known as 5G) is the introduction of mmWave frequency ranges, also referred to as Frequency Range 2 (FR2). The purpose of FR2 is to increase available capacity in specific areas, as FR2 system bands can support bandwidths up to 400 MHz that can be aggregated to 800 MHz. As a comparison, the maximum system bandwidth for FR1 is 100 MHz. FR2 currently includes two sub-frequency ranges. Bands n257, n258 and n261 range from 24.25 GHz to 29.50 GHz; and bands n259, n260 and n262 range from 37.00 GHz to 48.20 GHz.

This whitepaper highlights some of the challenges of integrating mmWave antenna solutions into different types of devices within the scope of 3GPP, with a focus on the smart phone form factor and extended reality (XR) glasses. The performance of the integrated antenna solutions is evaluated by simulations



of the device in a free space environment and while being gripped in different ways by the user. These simulations are then compared to the radiated performance requirements specified by 3GPP. The radiated performance of cellular wireless devices is very important for cell efficiency and coverage, and the aim of the 3GPP radiated requirements is to avoid designing devices that will have poor radiated performance.

mmWave inclusion in 5G NR

Operating at FR2 frequencies (such as 28 GHz or 39 GHz) will decrease the wavelength (10.7 mm @ 28 GHz and 7.7 mm @ 39 GHz) significantly compared to FR1 (for example, 11 cm @ 2.7 GHz). The effective antenna aperture (Aeff) for a given electrical length (for example, a $\frac{1}{4}$ wavelength) will also be significantly smaller. This can have an impact on the path loss, as explained below, and therefore has the potential to affect the obtained link budget for system bands operating at FR2 frequencies.

The propagation loss of an isotropic antenna is frequency independent, as the energy is spread equally on a sphere around the origin and depends on the transmit power and the distance from the transmit origin to the receive point (d). Assuming a reference power of 0 dB and isotropic transmit and receive antennas, the propagation loss can be expressed by the following equation.

Propagation loss of an isotropic antennas =
$$\frac{1}{4 * \pi * d^2}$$

The equation for propagation loss contains no frequency-dependent components and will have the same value for all frequencies. However, the effective antenna aperture is a function of the wavelength (λ) and the available gain (G) of the antenna, whereby the gain of an antenna is directly related to its physical size.

$$A_{eff} = \frac{G * \lambda^2}{4 * \pi}$$

This relation includes the frequency-dependent wavelength (λ) component and shows that the effective aperture of an antenna increases with the square of the wavelength, whereby antennas operating at lower frequencies have an inherent advantage in collecting the energy of propagating waves, since they are typically physically larger.

The transmission loss can be represented by the Friis Transmission Equation where the effective antenna aperture is expressed as antenna gain values (G_Tx & G_Rx), and the loss increases as the frequency increases for antennas with constant electrical length (constant antenna gain), such as monopole antennas.

$$P_{Rx} = P_{Tx} * G_{Tx} * G_{Rx} * \left(\frac{\lambda}{4 * \pi * d}\right)^2$$

As such, a ¼ wavelength antenna at FR1 will be able to receive and transmit energy more efficiently, because of its larger effective antenna aperture, compared to one at FR2 frequencies. The effective antenna aperture can be increased by using multiple elements in an array configuration, whereby the antenna will be more efficient in certain directions, but less efficient in other directions. This is expressed as antenna directivity (gain) and 3 dB radiation bandwidth (or half-power radiation bandwidth).



This is illustrated in Figure 1 for a distance between the two antennas of 1000 meters, where the propagation loss is derived from [1] to approximately 142 dB for all frequencies (purple curve). The path loss for unit-sized antennas at both the transmitter and receiver side (constant gain) is increasing as the frequency increases (blue curve), as derived by the Friis Transmission Equation. The pathloss is constant over frequency if the physical size of the antenna is also kept constant (increasing Aeff as the frequency increases, a factor of 4 for each time the frequency is doubled) at either the Tx or Rx side (red curve). The pathloss will decrease over frequency if the physical antenna size is kept constant at both the Tx and the Rx sides (yellow curve).

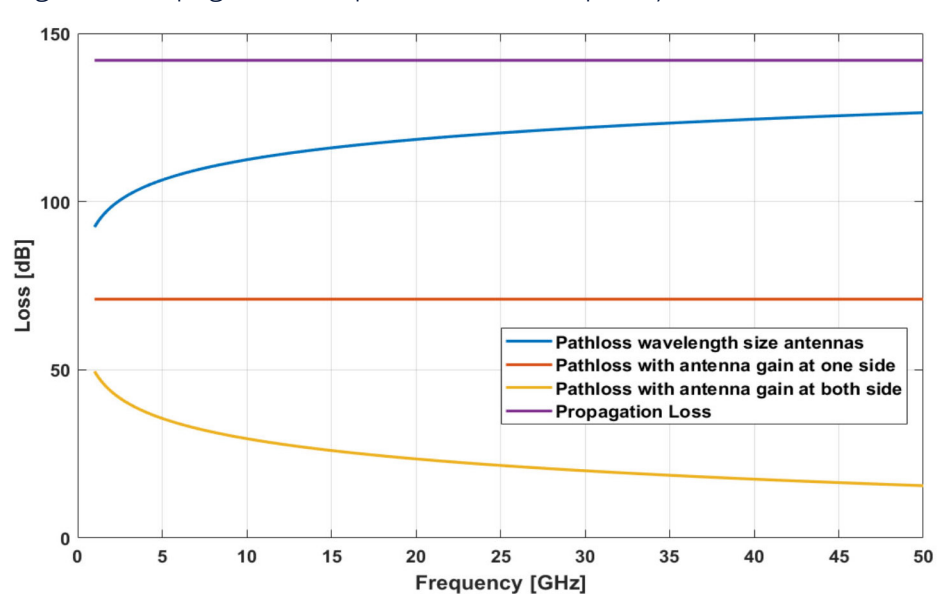


Figure 1: Propagation and pathloss over frequency at 1000 m distance.

A high-gain antenna array with narrow 3D radiation beamwidth is expected to be deployed at both the gNB (NR Base Station) and the User Equipment (UE), which is the term used by the 3GPP for a device. This increases the aperture of the antennas and improves the link budget at FR2 frequencies. A configuration like this can in theory even improve the link budget (Signal to Noise Ratio (SNR)), compared to the FR1 frequencies (yellow curve) if the physical size of the antennas used for FR2 frequencies is equal to the physical size of the antenna used for FR1 frequencies. However, such large antennas at FR2 frequencies are impractical, especially for handheld devices, and the obtained link budget performance for FR2 is expected to be in between the pathloss results for a configuration with wavelength-sized antennas at both sides (blue curve) and a configuration with high-gain antenna at one side (red curve).

However, this improvement in link budget will only be obtained if the beams at the gNB and the UE are aligned, which will require beam management between the gNB and the dynamically moving and rotating UE.



3GPP mmWave vision

6

The gNB \leftrightarrow UE beam alignment procedure in 5G New Radio (NR) Release 15 is described in [3GPP TR 38.802 section 6.1.6] and in [TS 38.214 section 5.2]. The beam alignment procedure includes three main phases, as described below, and illustrated in Figure 2.

Phase 1: The UE is assumed to be using a static beam for Rx reception, while the gNB is performing Downlink (DL) Synchronization Signal Block (SSB) beam sweeping (up to 64 beams). The static beam is typically a broad beam, but could also be an aligned narrow beam, depending on the capabilities of the UE. The Reference Signal Received Power (RSRP) is derived for all received SSB beams at the UE, and the SSB beam received with the highest RSRP level is identified. This best SSB beam (i.e., the one with the highest RSRP level) is associated with a specific Random Access CHannel (RACH) Opportunity (RO), which the UE will decode from the Master Information Block (MIB), System Information Block 1 (SIB1) and SIB2. The UE sends a preamble message (msg1) to that RO, where the gNB will be configured with the same spatial filter (beam) or a spatial filter covering the same angular area as used to transmit the SSB with the highest RSRP level. When the gNB receives a preamble at a specific RO, it will know which SSB beam is best for the specific UE.

Phase 2: The UE is still assumed to be configured with a static (broad) beam while the gNB is performing refined DL Channel State Information Reference Signal (CSI-RS) beam sweeping on the best SSB beam seen at the UE. The spatial filters used at the gNB for this refinement are either equal to the SSB beam or multiple beams with a narrower spatial filter, that together will cover the same spatial area as the SSB beam. The UE measures RSRP (or Channel Quality Indicator (CQI) or Rank Indicator (RI)) for all received CSI-RS beams and reports the best beam ID back to gNB with the same beam configuration used for receiving the CSI-RSs.

Phase 3: gNB transmits aperiodic CSI-RS with the best refined beam found in Phase 2 in a static configuration. This is indicated to the UE by setting the repetition index in the CSI-RS Information Element (IE) to "ON", whereby the UE knows it can use these CSI-RSs for narrow beam refinement.



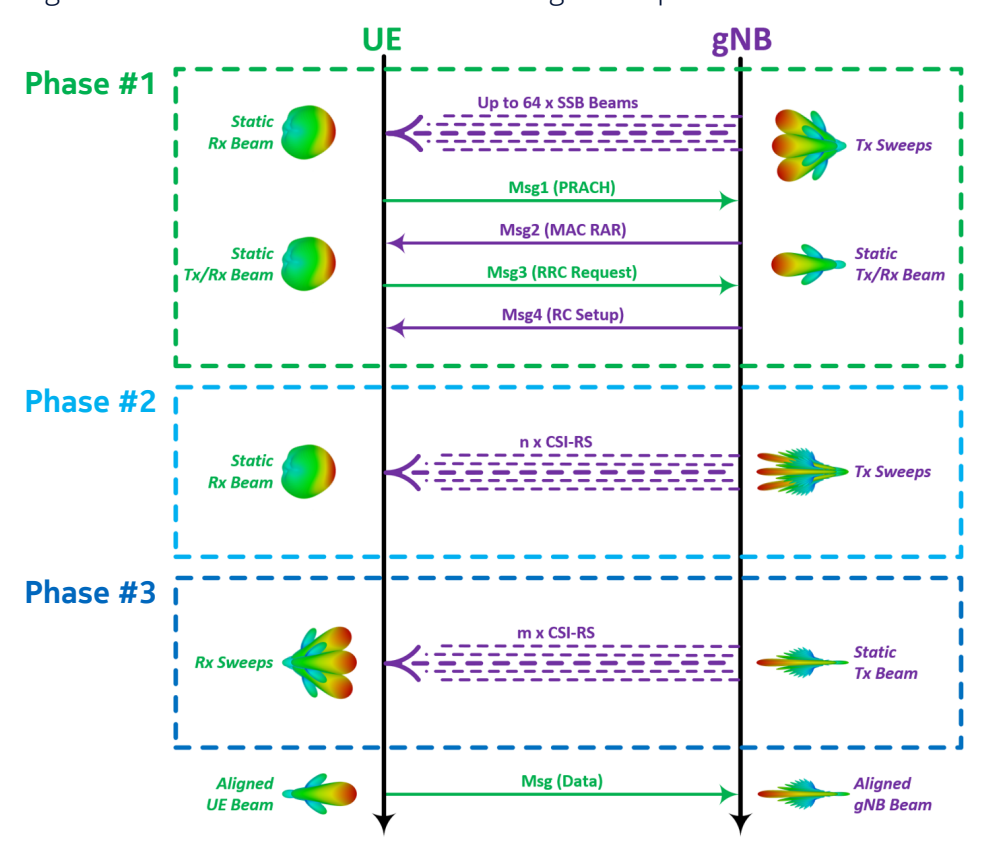


Figure 2: 5G NR 3GPP rel15 FR2 beam alignment procedure

At the end of Phase 3, alignment between the gNB Tx beam and the UE Rx beam is obtained in the downlink for maximized directional gain and minimum interference to other users in serving and neighboring cells.

The beam management at the UE is not specified by 3GPP, as this is considered specific to the UE implementation. In addition, the aperiodic CSI-RS with repetition "ON" is not a mandatory signal that the gNB must transmit. As such, beam refinement at the UE is up to the UE manufacturers, as a UE cannot rely on gNB assistance and is seen as a competitive factor that is not shared within the 3GPP community.

3GPP radiated performance requirements

7

3GPP has specified a requirement [TS 38.101-2] for the radiated performance for handheld UEs categorized as Power Class 3 (PC3). These specifications include a requirement for both transmitter-radiated power and receiver sensitivity. These requirements are based on Over the Air (OTA) measurements. This is new compared to FR1, where all 3GPP-specified measurements are conducted measurements.

The requirements for minimum peak Equivalent Isotropic Radiated Power (EIRP), Total Radiated Power (TRP) and EIRP spherical coverage can be found in TS 38.101-2, Table 6.2.1.3-1 to Table 6.2.1.3-3 [3], and are included in Table 1 as a reference.



Table 1: Summary of 3GPP requirements for radiated power for PC3

Operating band	Min peak EIRP (dBm)	Max TRP (dBm)	Max EIRP (dBm)	Min EIRP at 50%-tile CDF (dBm)
n257	22.4	23	43	11.5
n258	22.4	23	43	11.5
n259	18.7	23	43	5.8
n260	20.6	23	43	8.0
n261	22.4	23	43	11.5
n262	16.0	23	43	2.9
N263	14.1	23	43	2.3

The requirements for reference sensitivity power levels and Equivalent Isotropic Sensitivity (EIS) spherical coverage can be found in TS 38.101-2, Table 7.3.2.3-1 and Table 7.3.4.3-1³, and are included in Table 2 and 3 as a reference.

Table 2: Reference sensitivity for PC3

Operating	REFSENS (de	3m)/channel band	width				
band	50 MHz	100 MHz	200 MHz	400 MHz	800 MHz	1600 MHz	2000 MHz
n257	-88.3	-85.3	-82.3	-79.3	N/A	N/A	N/A
n258	-88.3	-85.3	-82.3	-79.3	N/A	N/A	N/A
n259	-84.7	-81.7	-78.7	-75.7	N/A	N/A	N/A
n260	-85.7	-82.7	-79.7	-76.7	N/A	N/A	N/A
n261	-88.3	-85.3	-82.3	-79.3	N/A	N/A	N/A
n262	-82.8	-79.8	-76.8	-73.8	N/A	N/A	N/A
n263	N/A	-78	N/A	-72	-69	-66	-65

Table 3: EIS spherical coverage for PC3

Operating	REFSENS (de	3m)/Channel band	lwidth				
band	50 MHz	100 MHz	200 MHz	400 MHz	800 MHz	1600 MHz	2000 MHz
n257	-77.4	-74.4	-71.4	-68.4	N/A	N/A	N/A
n258	-77.4	-74.4	-71.4	-68.4	N/A	N/A	N/A
n259	-71.9	-68.9	-65.9	-62.9	N/A	N/A	N/A
n260	-73.1	-70.1	-67.1	-64.1	N/A	N/A	N/A
n261	-77.4	-74.4	-71.4	-68.4	N/A	N/A	N/A
n262	-69.7	-66.7	-63.7	-60.7	N/A	N/A	N/A
N263	N/A	-66.2	N/A	-60.2	-57.2	-54.2	-53.2



5G NR device mmWave antenna implementation

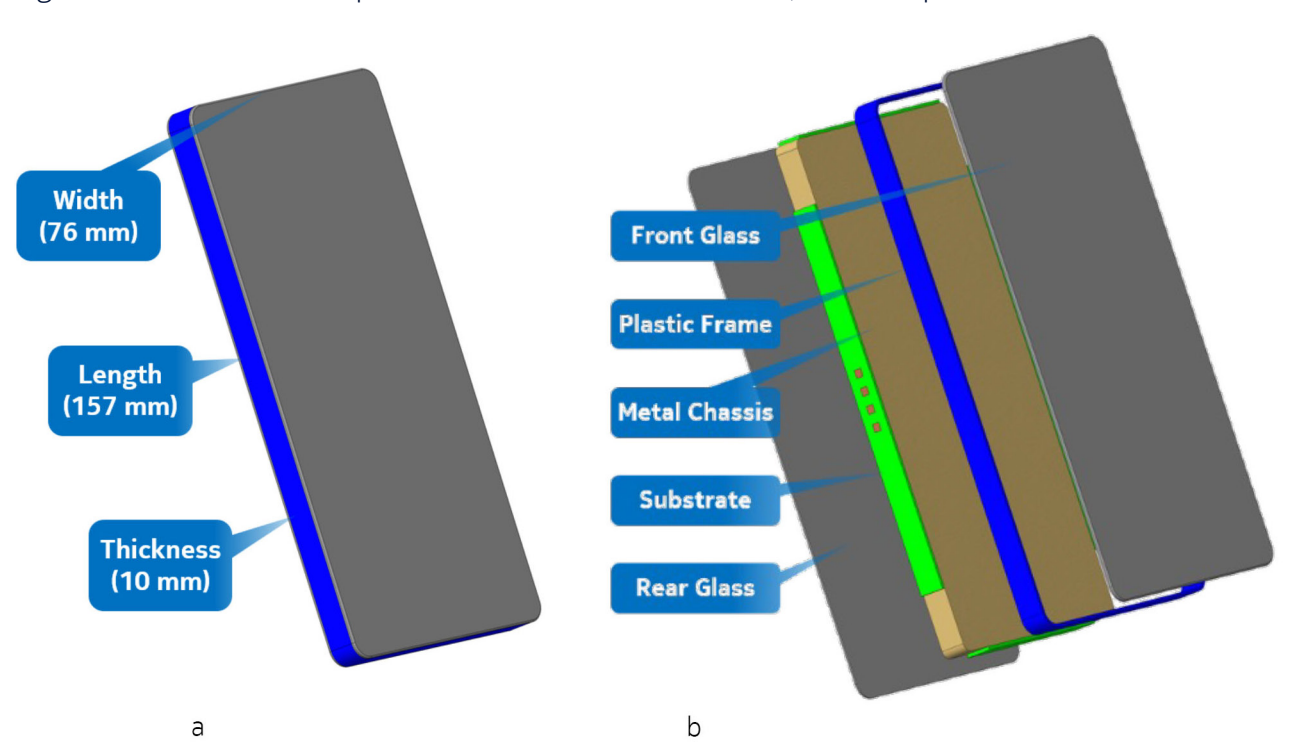
Due to the small wavelength at FR2 frequencies (10.7 mm @ 28 GHz and 7.7 mm @ 39 GHz) compared to the wavelengths at FR1 frequencies (33.3 cm @ 900 MHz and 11.1 cm @ 2700 MHz), the link budget will be significantly reduced if the antennas operating at FR2 frequencies are implemented with the same type of monopole antennas used for FR1 frequencies, as they will have a smaller aperture at FR2 frequencies. In addition, the monopole antennas at FR1 frequencies act more like couplers that excite the full form-factor chassis, or areas on the form-factor chassis, as the natural resonance of a typical smart phone form-factor chassis fits many of the frequencies utilized at FR1. As such, the antenna aperture at FR1 is very large, and it is unrealistic to maintain such large antenna apertures at FR2 frequencies. The consequence of a reduced aperture would be a reduced link budget for FR2. The typical antenna implementation for FR2, seen in the industry and in the literature, is a 1x4 antenna array, where each device has two or three of these antenna arrays implemented in the industrial design. This improves the spherical coverage, since each 1x4 antenna array will have increased directivity compared to the typical antenna implementations for FR1.

Implementation in a smart phone

9

A reference smart phone design is used to illustrate a possible FR2 antenna array implementation to visualize the antenna characteristics and evaluate the expected performance.

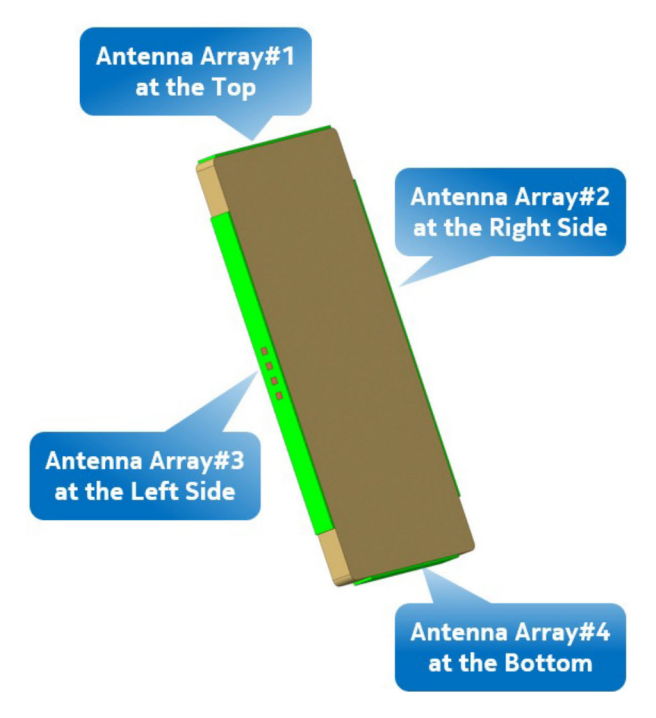
Figure 3: Reference smart phone form factor: a) dimensions; and b) Exploded view.





The placement of the four 1x4 antenna arrays implemented is shown in Figure 4. More or fewer antenna arrays could be selected, but four antenna arrays are used in this evaluation to illustrate a high-end device optimized for good performance. In addition, different placements of the antenna arrays are also possible, however the center placement has been chosen for this investigation to ensure that two or more antenna arrays will be affected by the user for the use cases that include the hand(s) of the user.

Figure 4: Placement of the implemented four 1x4 antenna arrays.



The performance is derived by creating electromagnetic simulations in the [CST Microwave Suite®] Electromagnetic software solver using the following electrical properties for the different materials used in the reference smart phone and for the simulations, including human hand phantoms.

Table 4: Material properties use for the CST simulations

Material properties @ 28 GHz	Dielectric constant	Loss tangent	Conductivity
Glass	5.75	0.0036	-
Plastic	2.90	0.075	-
Substrate	3.55	0.0027	-
Chassis	-	-	5.8*10 ⁷
Hand phantom	16.5	-	25.8

The material properties for the hand phantom are typically specified by [CTIA], which is currently the case for FR1 frequencies. However, neither CTIA nor 3GPP have released official material properties yet for hand phantom for frequencies above 6 GHz, including 28 GHz. The numbers used for these simulations represent the typical values used by the industry, universities, and research institutions.



Typical smart phone antenna performance

Within 3GPP, beam steering is assumed, at both the gNB and the UE, as illustrated in Figure 2. However, the number of antenna arrays and the number of configurable beams per antenna array are not specified by 3GPP. This evaluation will be made with four antenna arrays (as shown in Figure 4), where each antenna array can configure seven different beams (-45°, -30°, -15°, 0°, 15°, 30°, and 45°). The simulation results are only included for 28 GHz and for the Co-Polarized (Co-Pol) feeding of the antenna arrays. The performance of the Cross-Polarized (Cross-Pol) will be comparable to that of the Co-Pol results shown in terms of TRP and spherical coverage. However, the individual radiation patterns will be different if the patch elements used are aligned with a square orientation compared to the ground plane (see Figure 5 part a). The radiation patterns will be more equal if the patch elements are aligned with diamond orientation compared to the ground plane, since the edges of the patches are more symmetrical to the edges of the ground plane (see Figure 5 part b).

Figure 5: Orientation of the patch elements in the antenna array





A square orientation of the element patches is used for this reference smart phone design, as illustrated in Figure 4, and the following simulated radiation patterns are shown for Co-Pol only and limited to antenna arrays 1 and 2, to reduce the number of figures. In addition, only three beam configurations are shown per antenna array for four different use cases: Free Space (FS), Right Hand Browse (RHB), Dual Hand Browse (DHB) and Dual Hand Gamer (DHG). However, the performance analysis is performed for all four antenna arrays, including seven beams per antenna array.

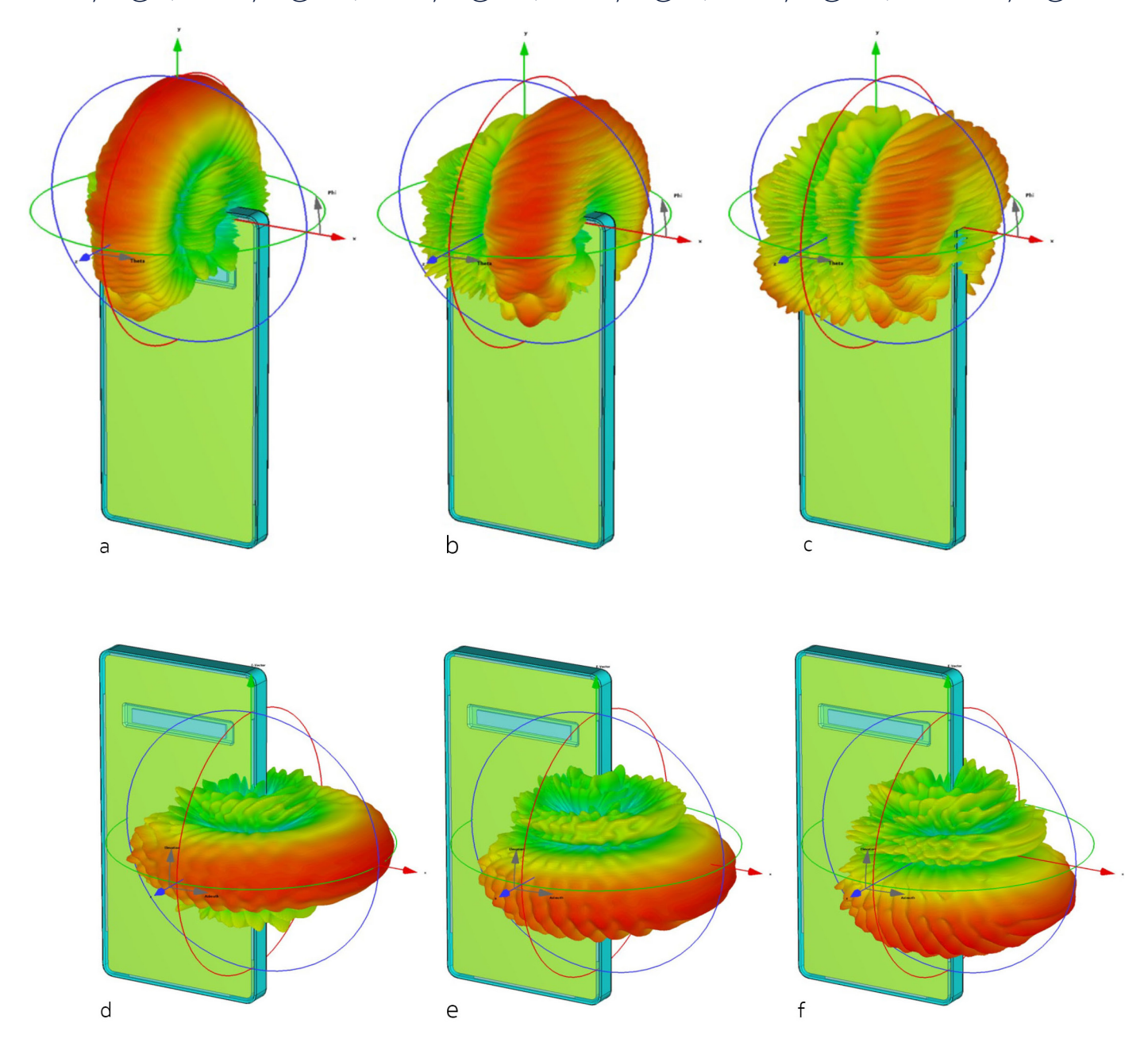
The hand phantom and the RHB grip used is specified by CTIA, while the DHB and DHG grips are defined by Nokia, since CTIA or 3GPP have not yet defined such grips.



Free space radiation patterns

Some of the simulated radiation patterns for the smart phone form factor in free space are shown in Figure 6.

Figure 6: Free Space beam configurations: a) Array 1 @ 0; b) Array 1 @ 15°; c) Array 1 @ 30°; d) Array 2 @ 0°; e) Array 2 @ 15°; and f) Array 2 @ 30°.

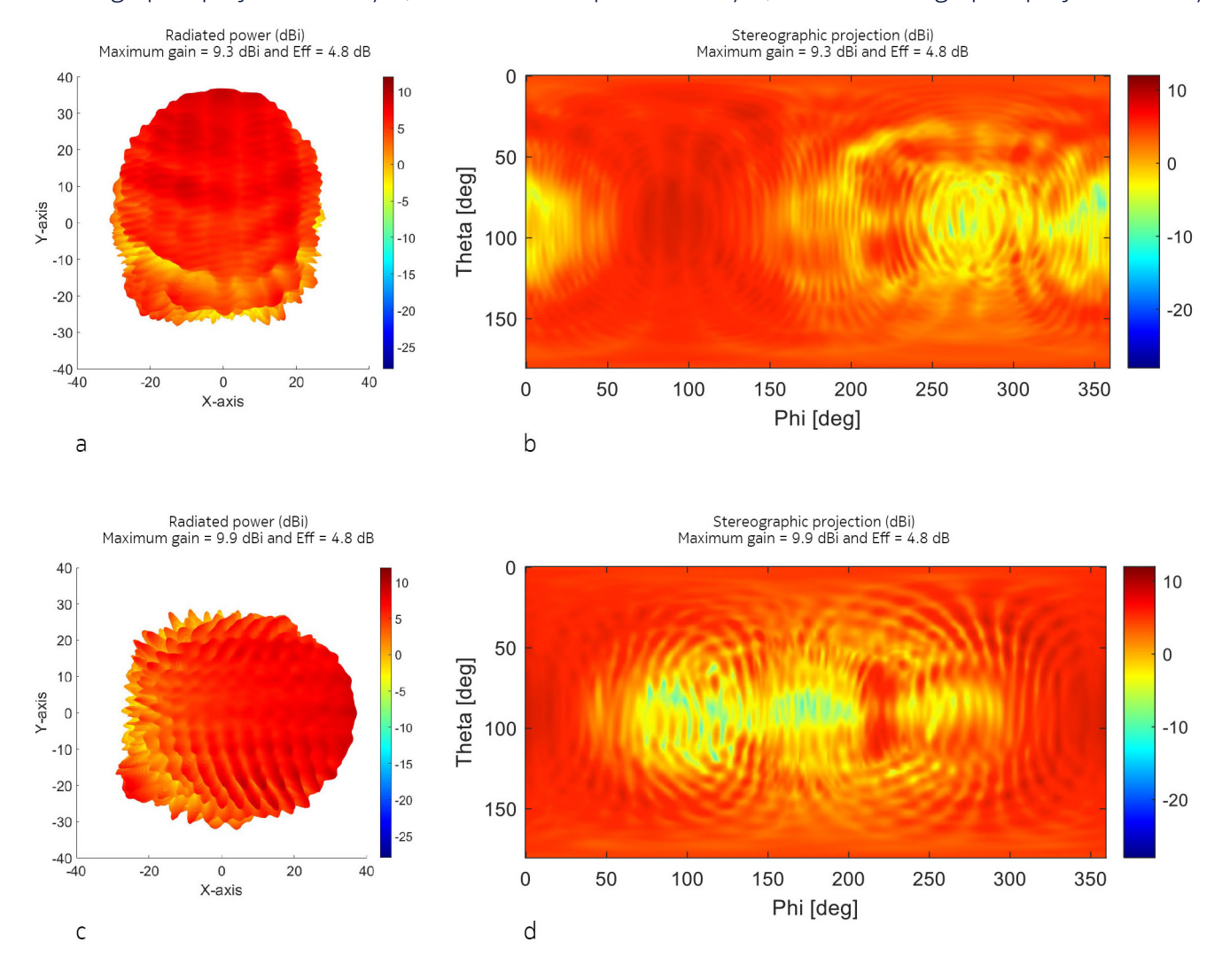




The radiation patterns are shown as gain values, so they exclude any potential loss due to impedance mismatch at the antenna array elements but include any absorption loss in the materials and applied hand phantoms used. The high amount of ripple observed for the radiation patterns is mostly caused by the front and rear glass acting as a waveguide at 28 GHz, where the energy coupled into the glass bounces forward and back creating standing waves. Some of the ripple is also coming from standing waves on the electrically large smart phone chassis.

The combined power envelope plot for all seven beam configurations is shown in Figure 7.

Figure 7: Combined power envelope of the 7 configurable beams in FS: a) 3D radiation pattern array 1; b) Stereographic projection array 1; c) 3D radiation pattern array 2; and d) Stereographic projection array 2.





The simulated maximum gain values for the different plots are summarized in Table 5.

Table 5: Simulated maximum antenna gain values for FS.

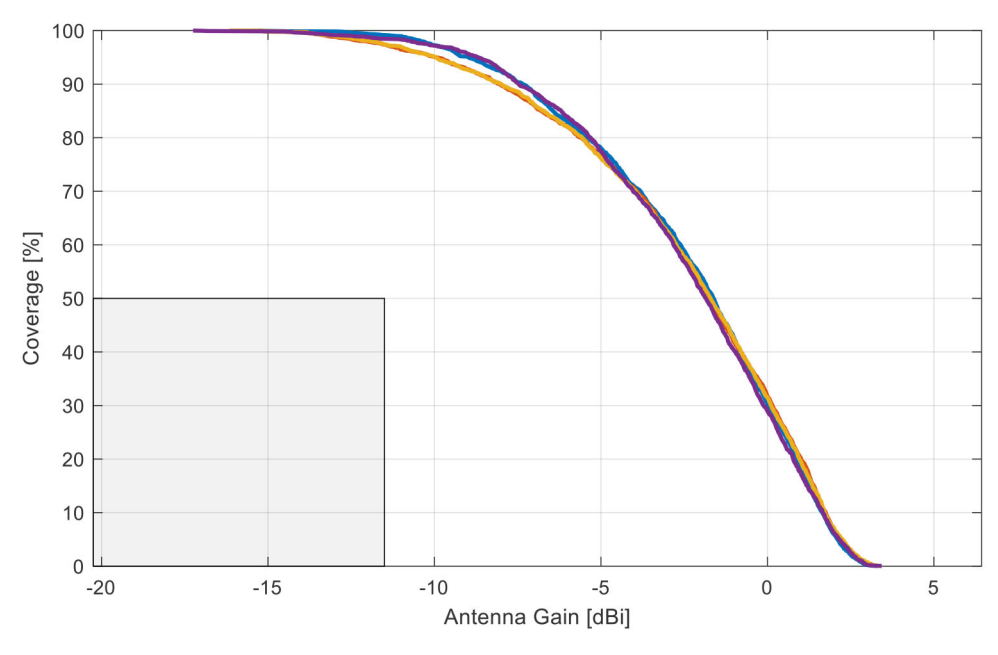
	Maximum	antenna gain valı	ues [dBi]					
Antenna	-45	-30	-15	0	15	30	45	
Array 1	7.7	8.7	9.0	9.3	8.9	8.3	7.2	
Array 2	9.2	9.9	9.0	9.3	9.0	8.8	8.2	
Array 3	9.2	9.9	9.0	9.3	9.0	8.8	8.2	
Array 4	7.9	9.6	8.8	9.1	8.6	8.1	7.3	

As shown in Table 5, the standing waves primarily introduced by the front and rear glass have an effect on the simulated maximum antenna gain values, as the highest antenna gain values are not always found for the boresight antenna array configuration, which is expected for a standalone antenna array.

Figure 8 shows the spherical FS antenna gain coverage for each individual antenna array, where an implementation loss of 6 dB has been added, and the conversion to antenna gain coverage from the 3GPP specified EIRP coverage assumes 23 dBm Power Amplifier (PA) power delivered to the antenna array (see section 2.2.6 for more information).

Figure 8: Spherical FS coverage for each individual antenna array

Antenna gain coverage for PC#3 (-11.5 dBm @ 50MHz) = (99, 97, 97, 100) % (PA = 23.0 dBm, loss = 6.0 dB and max antenna gain = 3.4 dBi)



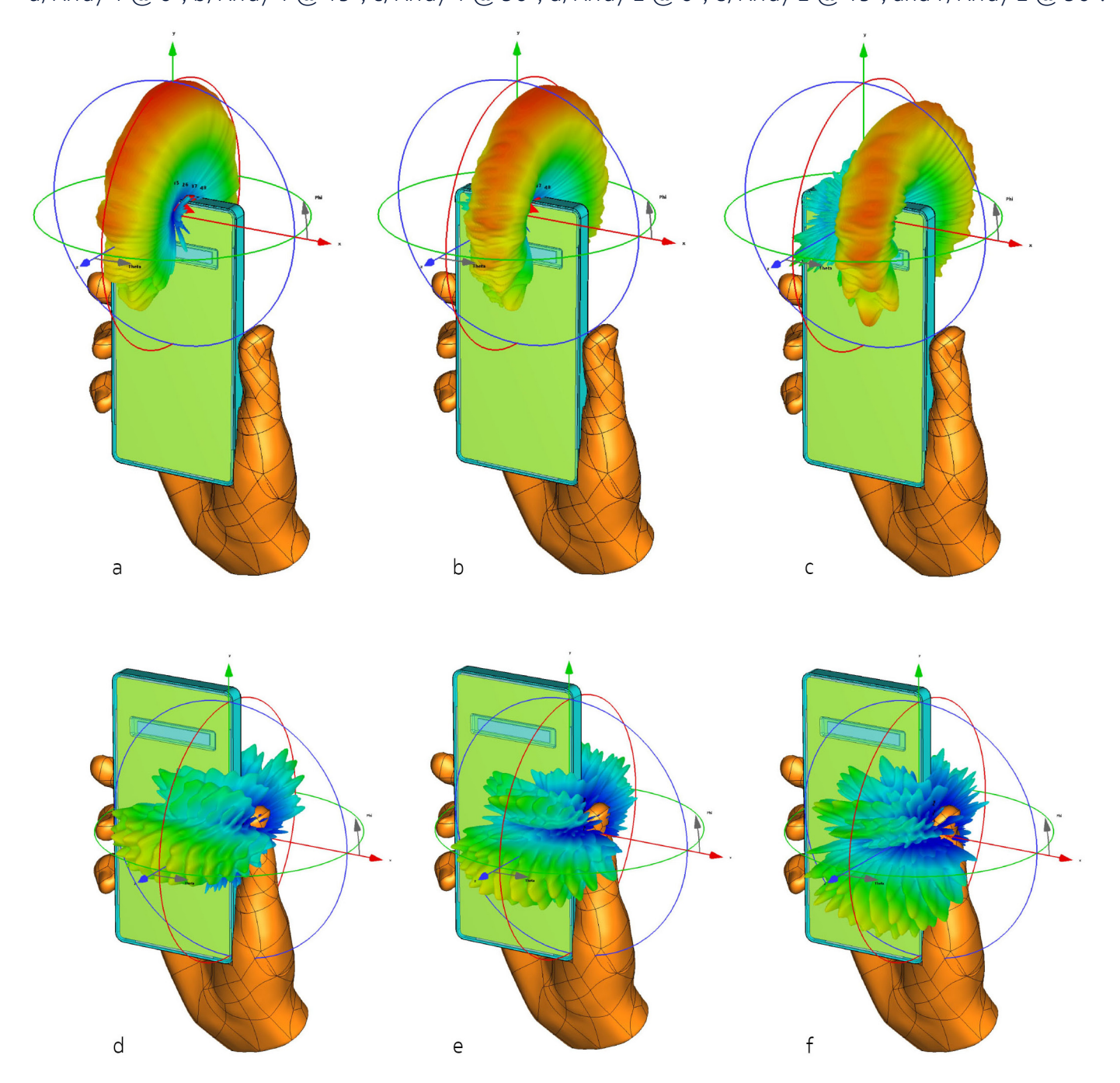
The difference in antenna gain coverage between the four antenna arrays in FS is very small. All four antennas perform equally well, and all antenna arrays are compliant with the 3GPP spherical coverage requirements (converted to antenna gain). The margin to the 3GPP requirements (grey box) is still around 10 dB, even with the added 6 dB implementation loss.



Right-hand browsing grip radiation patterns

Some of the simulated radiation patterns for the smart phone form factor with an added CTIA-defined right-hand browsing (RHB) grip phantom are shown in Figure 9.

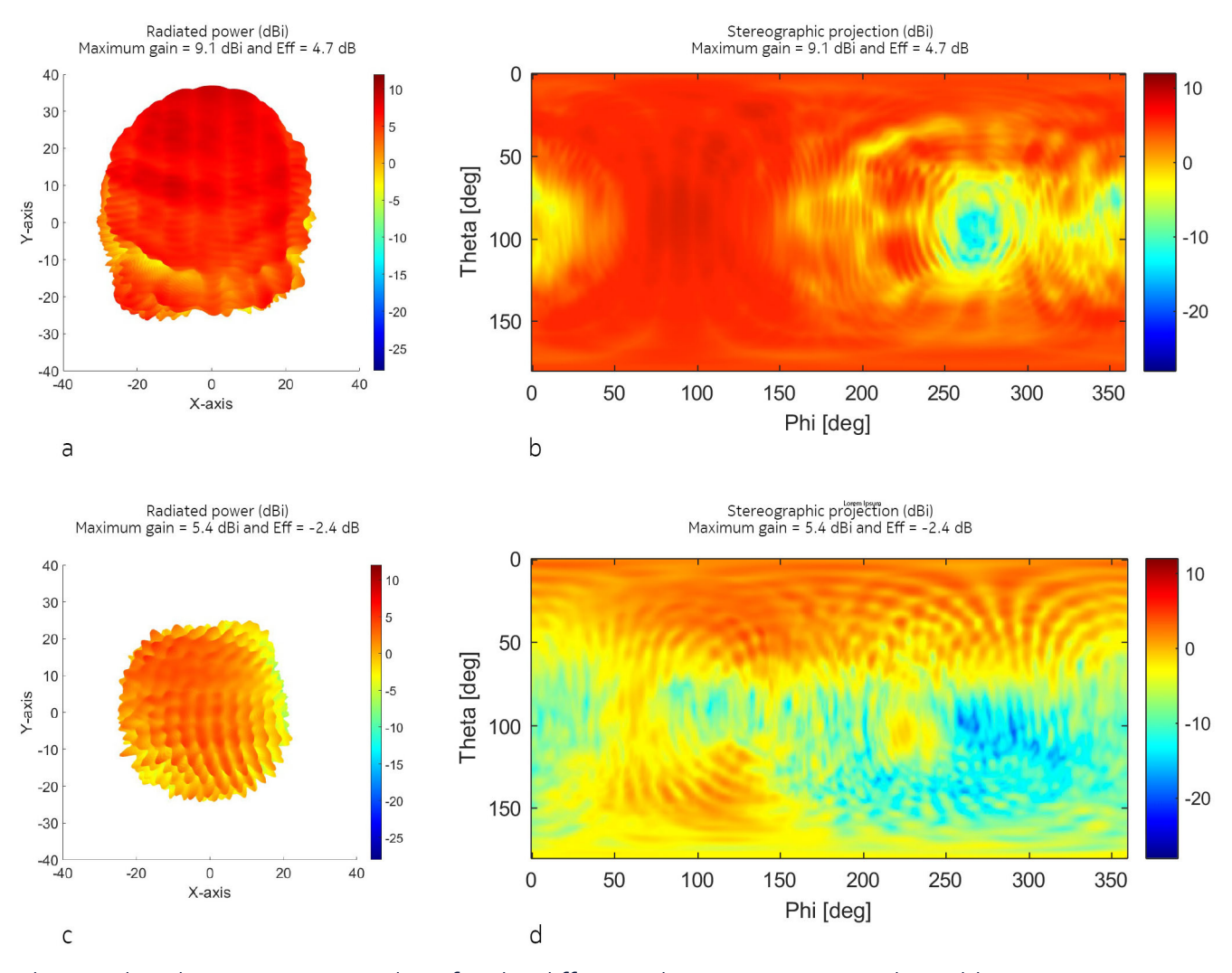
Figure 9: Right-hand browsing grip beam configurations:
a) Array 1 @ 0°; b) Array 1 @ 15°; c) Array 1 @ 30°; d) Array 2 @ 0°; e) Array 2 @ 15°; and f) Array 2 @ 30°.





The combined power envelope plot for all seven beam configurations is shown in Figure 10.

Figure 10: Combined power envelope of the 7 configurable beams for RHB grip: a) 3D radiation pattern array 1; b) Stereographic projection array 1; c) 3D radiation pattern array 2; and d) Stereographic projection array 2.



The simulated maximum gain values for the different plots are summarized in Table 6.

Table 6: Simulated maximum antenna gain values for RHB grip.

Maximum antenna gain values [dBi]								
Antenna	-45	-30	-15	0	15	30	45	
Array 1	7.7	8.4	8.9	9.1	8.7	8.2	7.1	
Array 2	3.2	4.2	4.7	4.5	4.1	5.4	3.5	
Array 3	6.1	8.0	7.1	7.3	7.4	8.6	7.1	
Array 4	8.0	9.7	9.5	9.9	9.6	9.1	6.9	

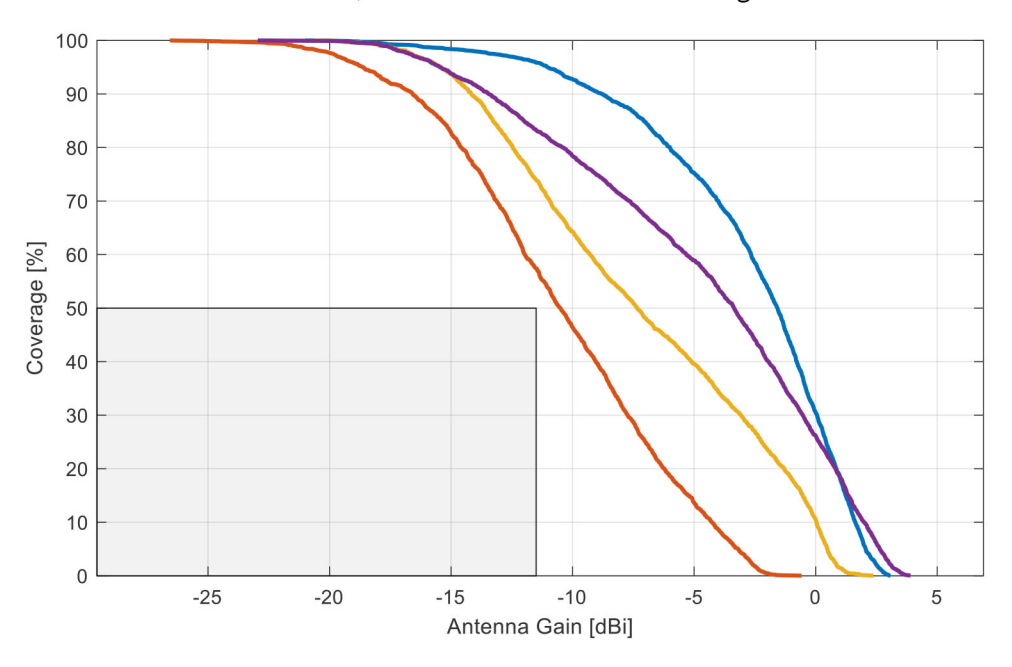
The data shown in Table 6 makes it clear that the user's hand has a large influence on the achieved antenna gain for the different beam configurations of the antenna arrays.



The spherical RHB antenna gain coverage for each individual antenna array is shown in Figure 11, with an added implementation loss of 6 dB.

Figure 11: Spherical RHB coverage for each individual antenna array

Antenna gain coverage for PC#3 (-11.5 dBm @ 50MHz) = (96, 57, 74, 83) % (PA = 23.0 dBm, loss = 6.0 dB and max antenna gain = 3.9 dBi)



Blue curve Red curve Yellow curve Spherical coverage of antenna array 1 Spherical coverage of antenna array 2 Spherical coverage of antenna array 3

Yellow curve Spherical coverage of antenna array 3
Purple curve Spherical coverage of antenna array 4

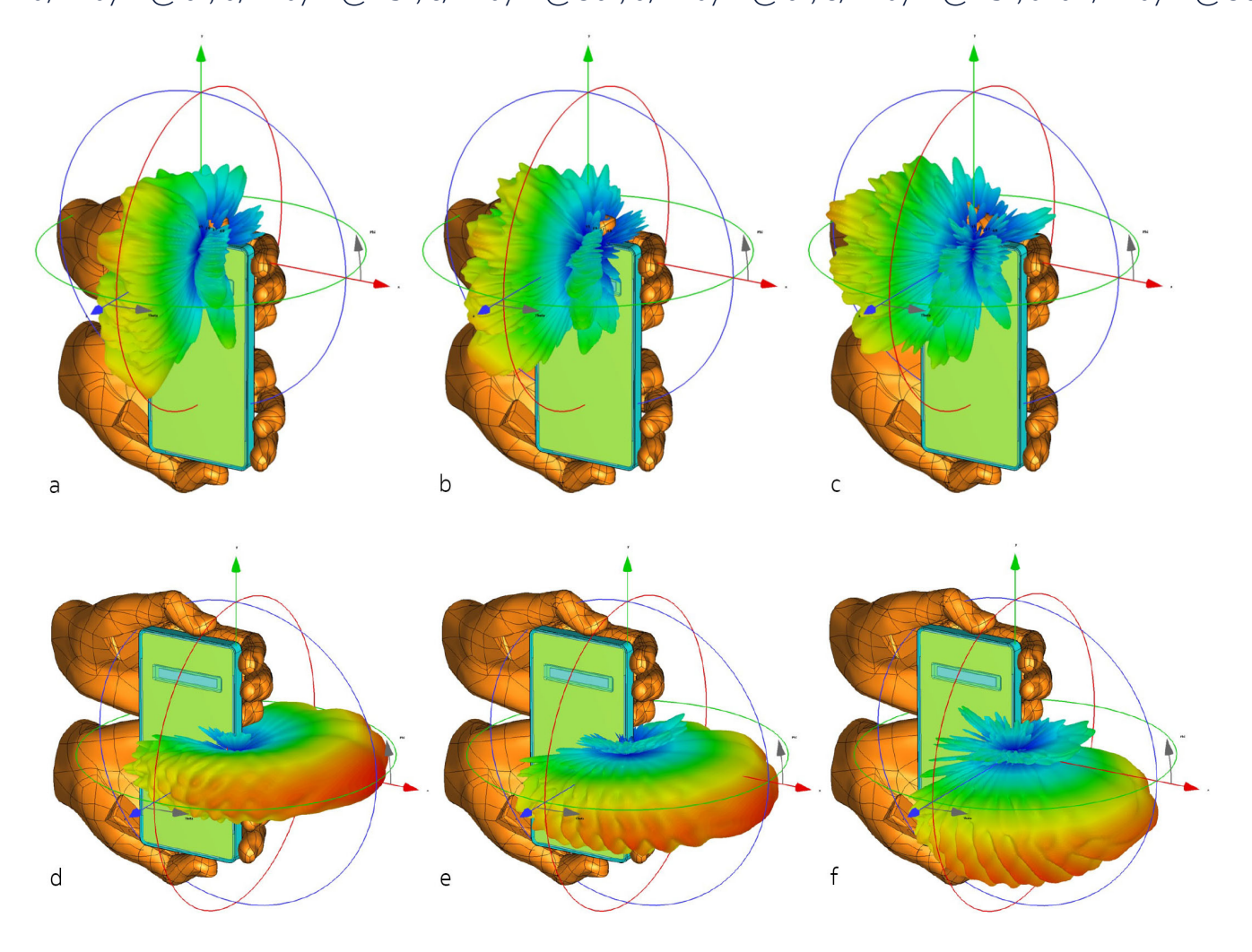
Compared to FS, the difference in antenna gain coverage between the four antenna arrays when including a RHB grip is now significant, where each antenna array achieves different performance levels. The performance of antenna array 1 is similar to the performance in FS (99% vs 96% coverage), as the hand is far away from that antenna array. The performance of antenna array 2 is the worst (57% coverage) as the thumb of the RHB grip is directly on top of that antenna array. The performance of antenna arrays 3 and 4 is in between the performance of antenna array 1 and 2, both of which are influenced by the fingers of the hand phantom. However, each individual antenna array is still compliant with the 3GPP spherical coverage requirements (gray box), even with the added 6 dB implementation loss and the CTIA right-hand browsing phantom.



Dual-hand browsing grip radiation patterns

Some of the simulated radiation patterns for the smart phone form factor, with an added Nokia-defined dual-hand browsing (DHB) grip phantom, are shown in Figure 12.

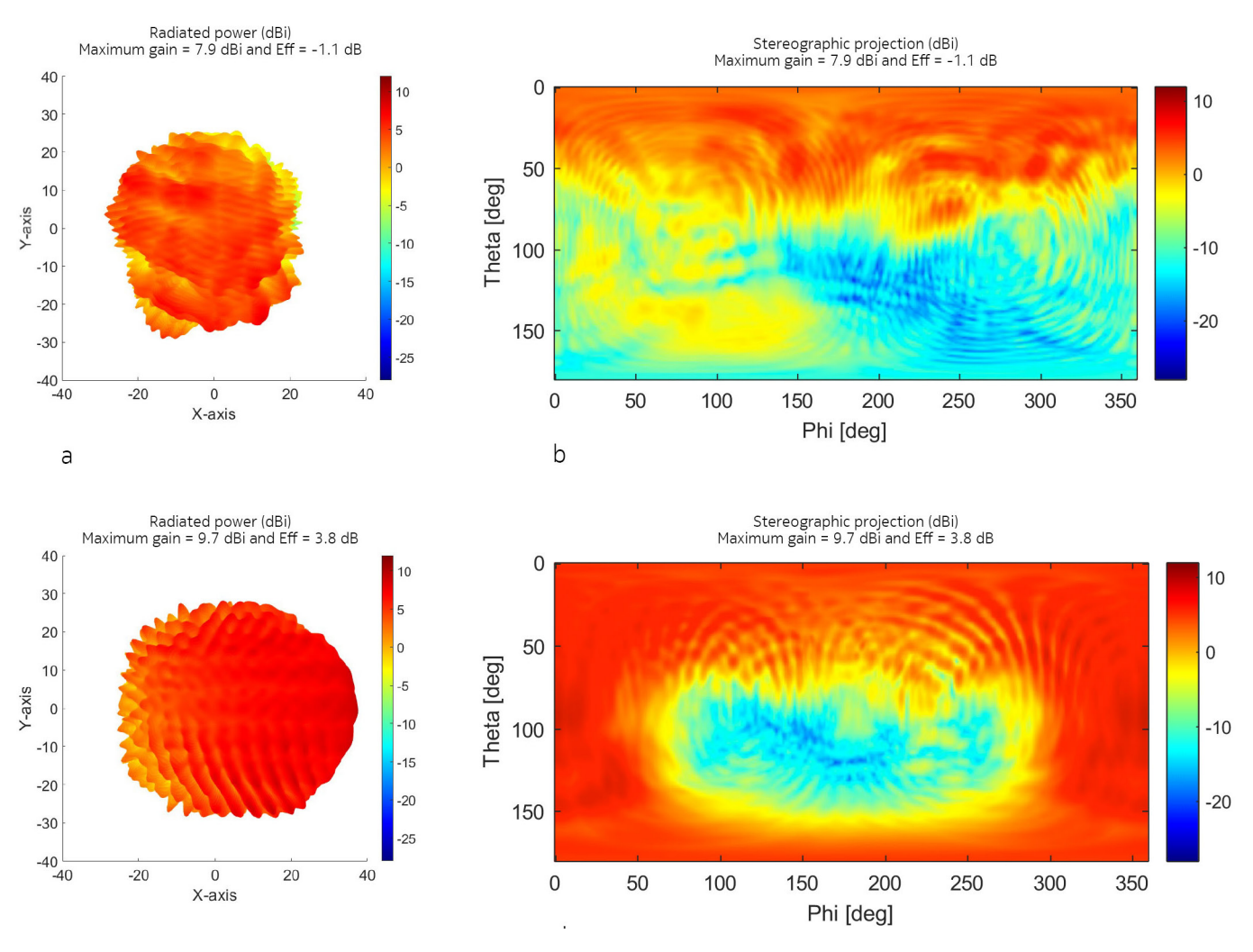
Figure 12: Dual-hand browsing grip beam configurations:
a) Array 1 @ 0°; b) Array 1 @ 15°; c) Array 1 @ 30°; d) Array 2 @ 0°; e) Array 2 @ 15°; and f) Array 2 @ 30°.



The combined power envelope plot for all seven beam configurations is shown in Figure 13.



Figure 13: Combined power envelope of the 7 configurable beams for DHB grip: a) 3D radiation pattern array 1; b) Stereographic projection array 1; c) 3D radiation pattern array 2; and d) Stereographic projection array 2.



The simulated maximum gain values for the different plots are summarized in Table 7.

Table 7: Simulated maximum antenna gain values for DHB grip

Maximum antenna gain values [dBi]								
Antenna	-45	-30	-15	0	15	30	45	
Array 1	7.1	6.8	6.9	6.8	6.2	7.9	6.3	
Array 2	9.0	8.8	9.1	9.6	9.0	8.9	7.8	
Array 3	11.3	11.7	10.7	11.5	11.1	10.3	8.8	
Array 4	5.9	6.1	5.6	6.1	6.3	7.6	6.6	

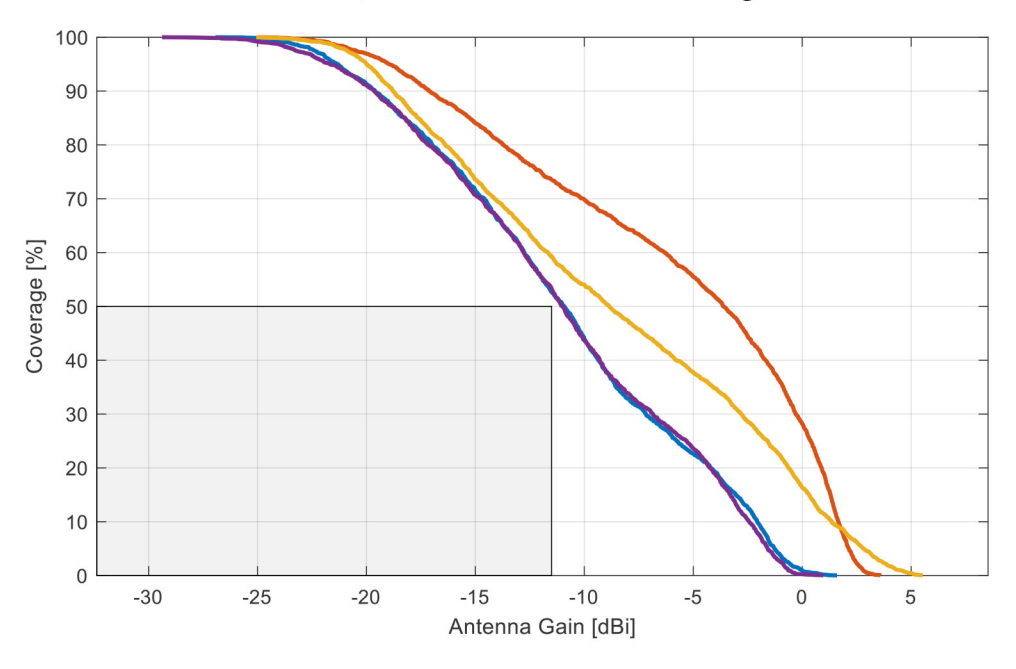


The observed antenna gains for antenna array 3 are very high for this use case, even 1 to 2 dB higher than the results for FS. This added antenna gain is due to the reflective properties of the hand phantom at these frequencies and because the electrical large area of the palms of the hand are within one or two wavelengths from the antenna array. Antenna array 1 and 4, where the thumbs are directly on top of (in the near-field) the antenna array perform worse.

Figure 14 shows the spherical DHB antenna gain coverage for each individual antenna array, with an added implementation loss of 6 dB.

Figure 14: Spherical DHB coverage for each individual antenna array

Antenna gain coverage for PC#3 (-11.5 dBm @ 50MHz) = (52, 73, 59, 53) % (PA = 23.0 dBm, loss = 6.0 dB and max antenna gain = 5.5 dBi)



Blue curve Red curve Purple curve Spherical coverage of antenna array 4

Spherical coverage of antenna array 1 Spherical coverage of antenna array 2 **Yellow curve** Spherical coverage of antenna array 3

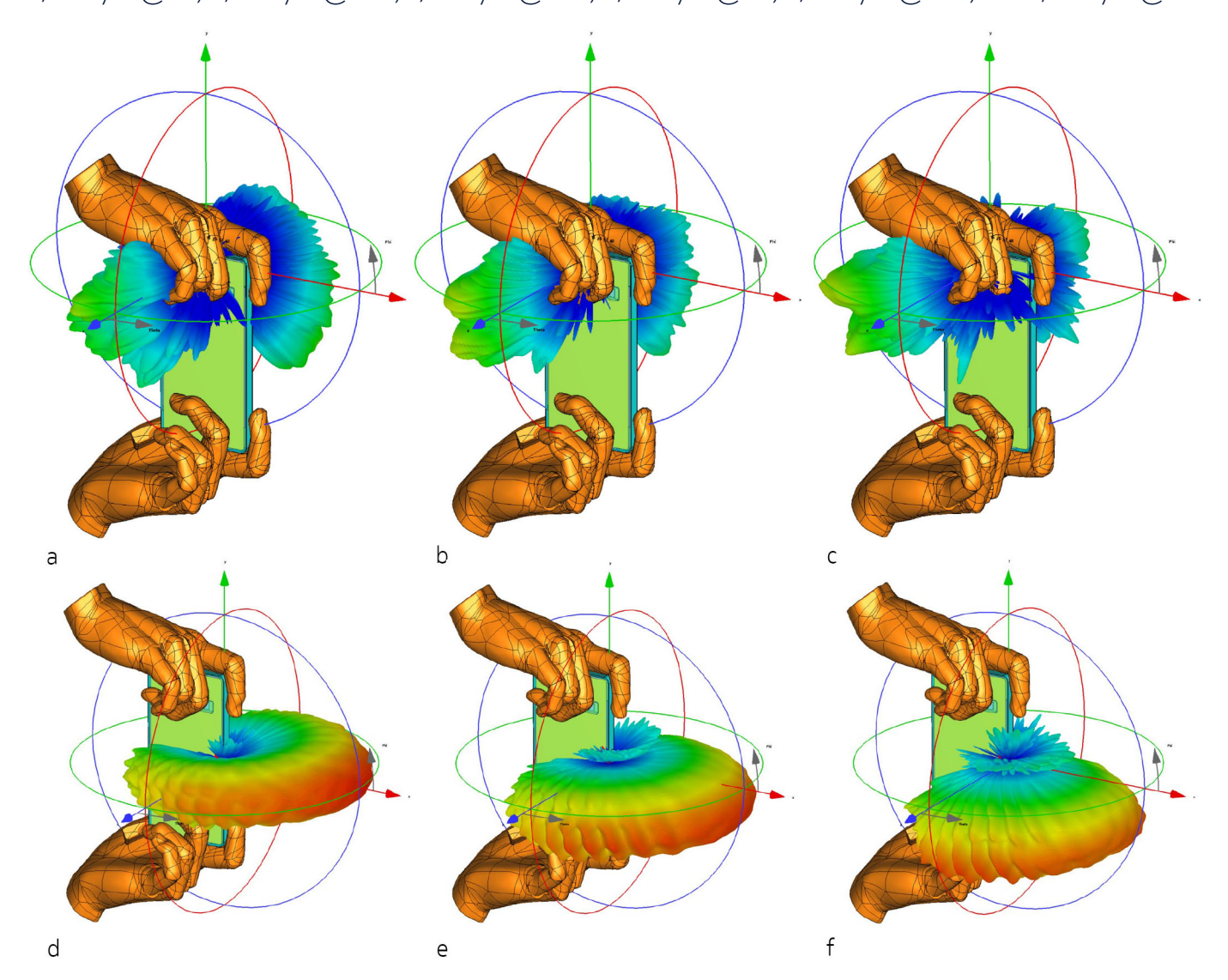
Compared to FS, the difference in antenna gain coverage between the four antenna arrays when including a DHB grip is also significant for this use case, where each antenna array achieves different performance levels. The performance of antenna array 2 is the best, with a spherical coverage of 73%, whereas the worst performance is seen for antenna arrays 1 and 4, at around 52 % spherical coverage. The performance results show again that the closer the parts of the hand are to an antenna array, the worse the performance is. However, each individual antenna array is still compliant with the 3GPP spherical coverage requirements (gray box), even with the added 6 dB implementation loss and the Nokia dual-hand browsing phantom.



Dual-hand gamer grip radiation patterns

Figure 15 shows some of the simulated radiation patterns for the smart phone form factor with an added Nokia-defined dual-hand gamer (DHG) grip phantom.

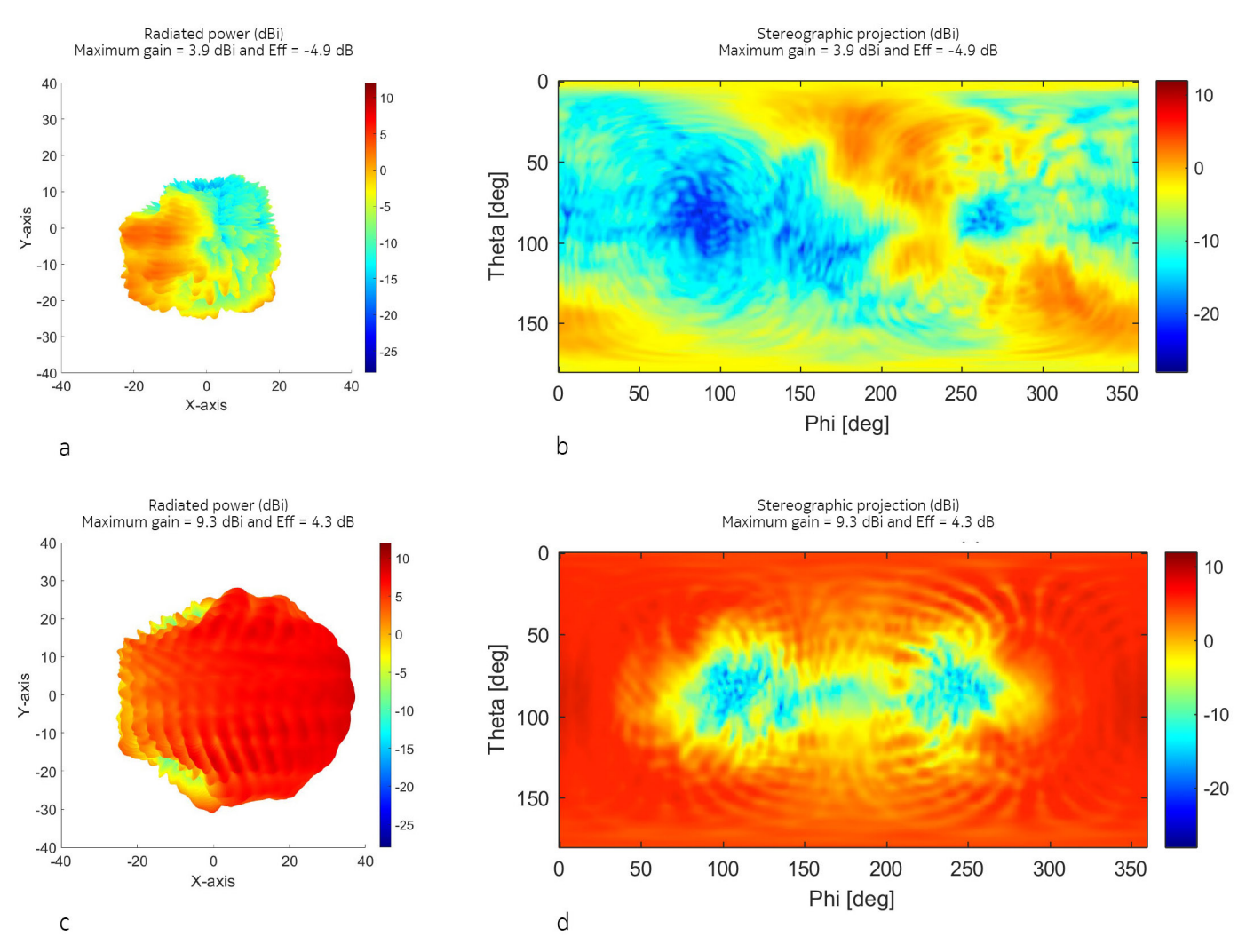
Figure 15: Dual-hand gamer grip beam configurations:
a) Array 1 @ 0°; b) Array 1 @ 15°; c) Array 1 @ 30°; d) Array 2 @ 0°; e) Array 2 @ 15°; and f) Array 2 @ 30°.



The combined power envelope plot for all seven beam configurations is shown in Figure 16.



Figure 16: Combined power envelope of the 7 configurable beams for DHG grip: a) 3D radiation pattern array 1; b) Stereographic projection array 1; c) 3D radiation pattern array 2; and d) Stereographic projection array 2.



The simulated maximum gain values for the different plots are summarized in Table 8.

Table 8: Simulated maximum antenna gain values for DHG grip

Maximum antenna gain values [dBi]								
Antenna	-45	-30	-15	0	15	30	45	
Array 1	2.2	3.2	3.4	2.4	2.9	3.9	3.5	
Array 2	7.4	8.8	8.9	9.3	8.9	8.3	7.4	
Array 3	7.8	8.6	9.0	9.2	9.0	8.0	7.2	
Array 4	1.9	3.3	3.4	3.0	3.4	3.9	3.5	

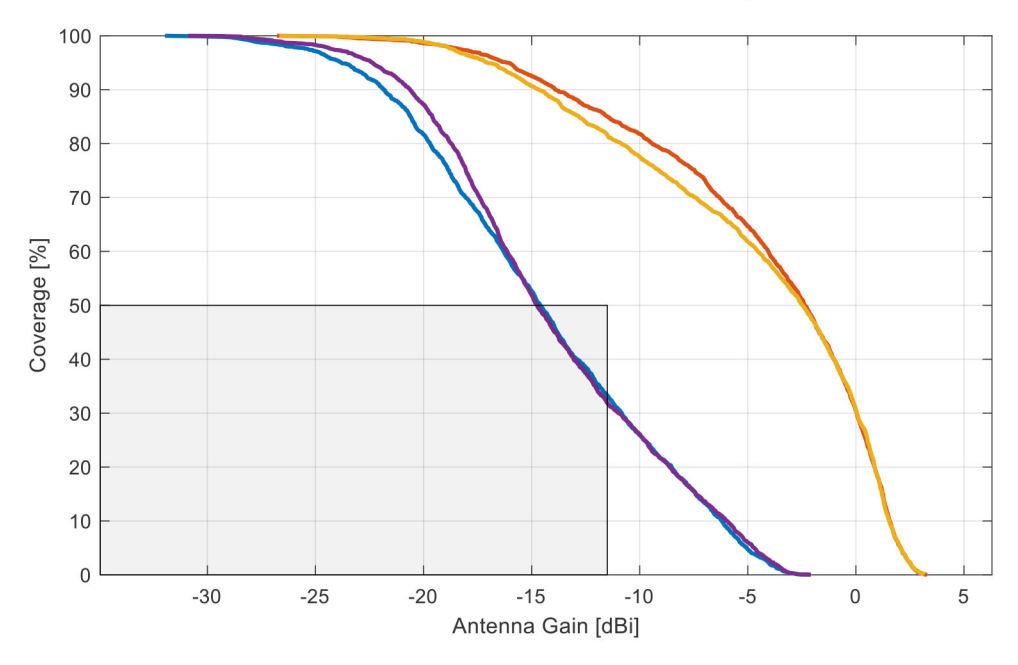
The data shown in Table 8 makes it clear that the user hand has a large influence on the antenna gain achieved by the different beam configurations of the antenna arrays.



The spherical DHG antenna gain coverage for each individual antenna array is shown in Figure 17, with an added implementation loss of 6 dB.

Figure 17: Spherical DHG coverage for each individual antenna array.

Antenna gain coverage for PC#3 (-11.5 dBm @ 50MHz) = (52, 73, 59, 53) % (PA = 23.0 dBm, loss = 6.0 dB and max antenna gain = 5.5 dBi)



Blue curveSpherical coverage of antenna array 1Red curveSpherical coverage of antenna array 2Yellow curveSpherical coverage of antenna array 3Purple curveSpherical coverage of antenna array 4

The difference in antenna gain coverage between the four-antenna arrays when including a DHG grip is still significant for this use case, where the performance of antenna array 2 and 3 are close to the FS performance, with spherical coverage values around 85%. Antenna array 1 and 4 on the other hand perform very poorly (spherical coverage \approx 33%) with this hand grip, as these antenna arrays are fully covered by the thumbs of the two hands. Only antenna array 2 and 3 are compliant with the 3GPP spherical coverage requirements (gray box) for this use case.



Radiated efficiency

The Total Radiated Efficiency (TRE) values for antenna arrays 1 and 2 are shown in Table 9 for different use cases with boresight beam configuration. The data in Table 9 shows that the absorption loss introduced by the interaction of the hand phantom of the user is relatively low, even for aggressive hand grips like the Gamer grip. These results are very different compared to FR1 (see Table 13) where much higher absorption losses are observed. The penetration depth of the human skin is very small at FR2 frequencies, and the conductivity of the human skin is higher at FR2 (25.8 S/m) compared to around 1.0 S/m at FR1 (1900 MHz), which makes the human tissue act as a reflector at FR2 instead of an absorber, as it does for FR1. The power radiated toward the hand is now mostly reflected instead of being absorbed. The reduction in efficiency is mostly introduced when the hand phantom is very close (≈1mm) to the elements of the antenna array, where the strength of the E- and H-fields are very high. This occurs mostly when the fingers of the hand phantom are right on top of the antenna arrays. Antenna array 1 is almost unaffected by the RHB grip, as the hand phantom is far away from the antenna element, and the effective antenna aperture is concentrated in the near vicinity of the physical antenna array.

Table 9: Examples of simulated TRE for different FR2 antennas and different use cases

	Total radiation e	Total radiation efficiency (Gain)				
Antenna	Free space	Right hand	Dual hand	Gamer grip	Maximum delta	
Array#1	-0.2 dB	-0.2 dB	-5.0 dB	-8.5 dB	8.3 dB	
Array#2	-0.2 dB	-5.9 dB	-0.6 dB	-0.6 dB	5.7 dB	
Array#3	-0.2 dB	-2.1 dB	-1.9 dB	-0.3 dB	1.9 dB	
Array#4	-0.2 dB	-0.7 dB	-5.1 dB	-8.5 dB	8.3 dB	

An implementation loss of between 4 dB and 8 dB is expected for these types of antenna array designs, as the array itself consists of a multi-layer stack-up with many traces and vias. In addition, the impedance mismatch on each element will also contribute to the loss. An implementation loss of 6 dB has been assumed in the following evaluation of the 3GPP requirements.

Larger sized antenna arrays are less sensitive to user interaction, as the user has less risk of covering all or most of the elements in the antenna array. As shown in Table 9, TRE values simulated for a 1x8 antenna array, instead of a 1x4 antenna array, are up to 2.0 dB better.



Max peak EIRP and spherical coverage

The maximum EIRP for boresight configuration in FS can be derived from the simulated maximum antenna gain values shown in Table 5, using the following assumptions:

- Power delivered to the antenna array is 23 dBm from the PA.
- An implementation loss of 6 dB is added to represent a realistic antenna array design integrated into a real smart phone industrial design.

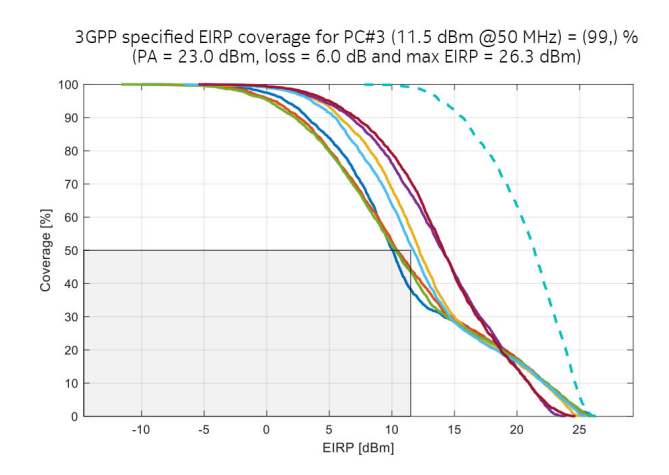
The maximum Peak EIRP values for antenna arrays 1 and 2 are derived from simulations to the following values:

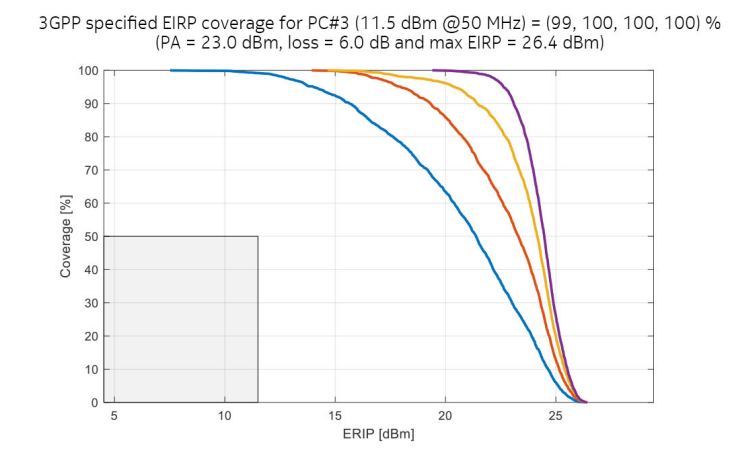
- 26.3 dBm for antenna array 1
- 26.7 dBm for antenna array 2

Both antenna arrays are compliant with the required minimum peak EIRP of 22.4 dBm as specified by 3GPP for a PC3 UE (see Table 1).

The spherical FS EIRP coverage is shown for the power envelope of antenna array 1 alone, including the individual seven beams, and for the combined power envelope of antenna arrays 1 and 2, antenna arrays 1, 2 and 3, and antenna arrays 1, 2, 3 and 4. The 3GPP spherical requirement (see Table 1) for EIRP is illustrated in Figure 18 with the gray box in each plot.

Figure 18: Spherical FS EIRP coverage CCDF curves: a) antenna array 1 including the 7 individual beams; and b) Combined power envelope of different antenna array combinations.





Solid curves figure a

Dashed curves figure a

Blue curve figure b

Red curve figure b

Yellow curve figure b Purple curve figure b Individual beams

Dashed curves figure a Combined power envelope

Power envelope of antenna array 1 alone Power envelope of antenna array 1 and 2 Power envelope of antenna array 1, 2 and 3 Power envelope of antenna array 1, 2, 3 and 4

The 3GPP spherical EIRP coverage requirements are also fulfilled for the implementation example, even if the smart phone is only implemented with a single 1x4 antenna array.



3GPP antenna and blocking models

Antennas are modeled in 3GPP Link Level Simulations (LLS) and System Level Simulations (SLS) according to the formulas documented in [3GPP, TR 38.803, Table 5.2.3.3], which specify the radiation pattern for a single antenna element. That radiation pattern can then be combined mathematically to create any beam-steered radiation pattern for any sized antenna array.

Table 10: UE antenna element pattern as defined by 3GPP

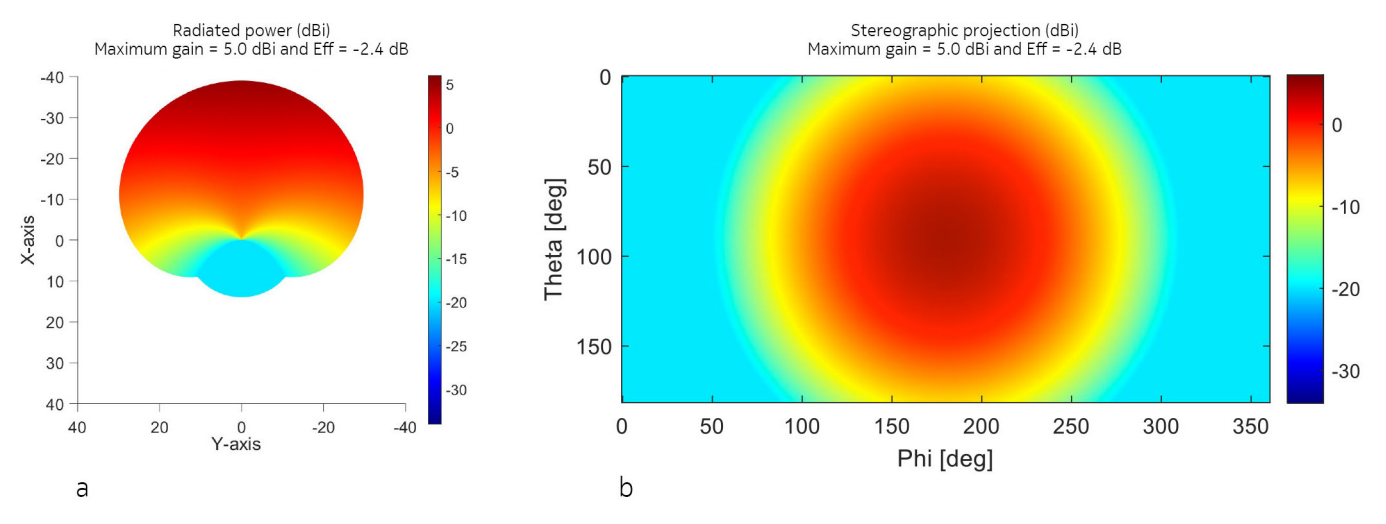
Antenna element vertical radiation pattern (dB)	$A_{E,V}(\theta'') = -\min\left\{12\left(\frac{\theta'' - 90^{\circ}}{\theta_{3dB}}\right)^{2}, SLA_{V}\right\}, \theta_{3dB} = 90^{\circ}, SLA_{V} = 25 dB$
Antenna element horizontal radiation pattern (dB)	$A_{E,H}(\varphi'') = -\min\left\{12\left(\frac{\varphi''}{\varphi_{3dB}}\right)^2, A_m\right\}, \varphi_{3dB} = 90^\circ, A_m = 25 dB$
Combining method for 3D antenna element pattern (dB)	$A''(\theta'', \varphi'') = -\min\left\{-\left[A_{E,V}(\theta'') + A_{E,H}(\varphi'')\right], A_m\right\}$
Maximum directional gain of an antenna element <i>GE,max</i>	5 dBi
(Mg, Ng, M, N, P)	(1, 1, 2, 2, 2)
(dv, dh)	(0.5λ, 0.5λ)
UE orientation	Random orientation in the azimuth domain: uniformly distributed between -90 and 90 degress* Fixed elevation: 90 degrees

*NOTE: This is done to emulate two panels: the configuration is equivalent to 2 panels with 180shift in horizontal orientation and UE orientation uniformly distributed in the azimuth domain between -180 and 180 degress



The element radiation pattern is visualized in Figure 19, as a 3D radiation pattern and as a stereographical projection.

Figure 19: Visualization of the 3GPP specified radiation pattern for a single antenna element: a) 3D radiation pattern; and b) stereographical projection.



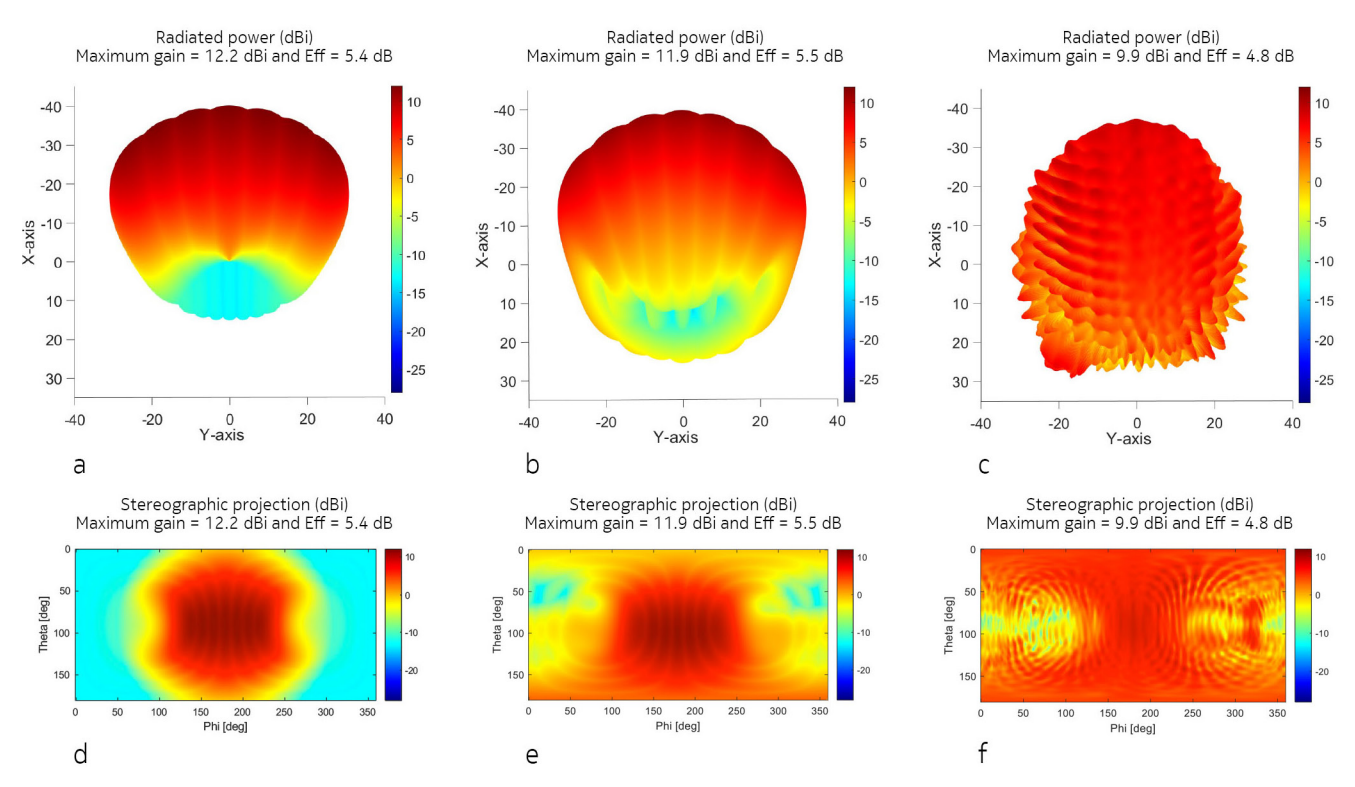
It is well accepted that this antenna approximation used within 3GPP for LLS and SLS simulation is not necessarily a correct representation of the radiation pattern obtained on a real smart phone deployed in a 5G NR network. However, since all devices will have different antenna characteristics, this approximation may be a valid compromise that is very easy to implement in any LLS and SLS code, as it is purely defined by mathematical formulas.

However, some significant differences are observed between the 3GPP model and the simulated radiation pattern derived from this reference smart phone form factor. Some of these differences are shown in the following figures (Figure 20 and Figure 21) as power envelope plots for a 1x4 antenna array with seven beams, based on the 3GPP specification, a stand-alone 1x4 antenna array, and a 1x4 antenna array on a reference smart phone form factor.

27



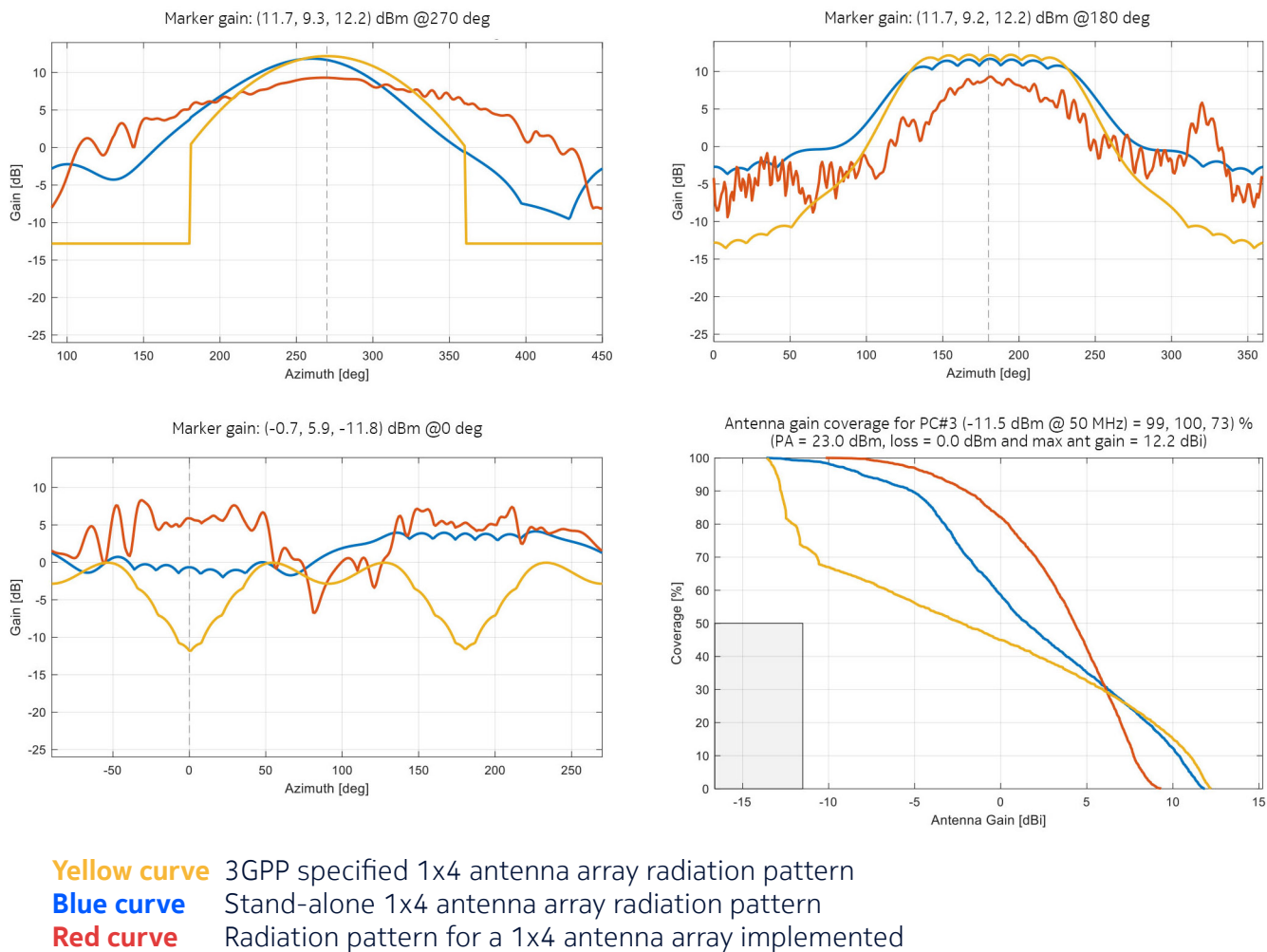
Figure 20: Single element radiation patterns: a and d) 3D Radiation patterns according to 3GPP; b and e) 3D Radiation patterns for a single element on a stand-alone 1x4 antenna array; and c and f) 3D Radiation patterns for a single element on a reference smart phone form factor.



These differences are easier to see on the three 2D cuts, as shown in Figure 21. Figure 21 also includes a spherical coverage plot (d) based on the derived/simulated antenna gain results. It assumes 23 dBm power delivered to the antenna and 0 dB implementation loss, as implementation loss is not directly included in the 3GPP antenna specifications.

NOSIA

Figure 21: 2D cuts of the combined power envelope: a) side view; b) front view; c) top view; and d) spherical antenna gain coverage.



on a reference smart phone form factor

As the 2D plots show, the antenna characteristics of the 3GPP model are more similar to those of a standalone 1x4 antenna array than they are to those of a 1x4 antenna array implemented on the reference smart phone form factor. The radiation energy is less directive for the 1x4 antenna array implemented on the reference smart phone form factor, than the 3GPP antenna model. This results in a lower maximum antenna gain, but a better coverage at the 3GPP-specified 50th percentile (gray box).



User interaction is defined within 3GPP as angular areas where an absorption loss of 30 dB is added to the FS radiation patterns, as shown in Figure 22 for a one-hand browsing grip, and in Figure 23 for a dual-hand browsing grip.

Figure 22: 3GPP blockage model for one-hand browsing grip: a) 3GPP model for antenna array 1; b) 3GPP model for antenna array 2; c) Simulated results for antenna array 1; and d) Simulated results for antenna array 2.

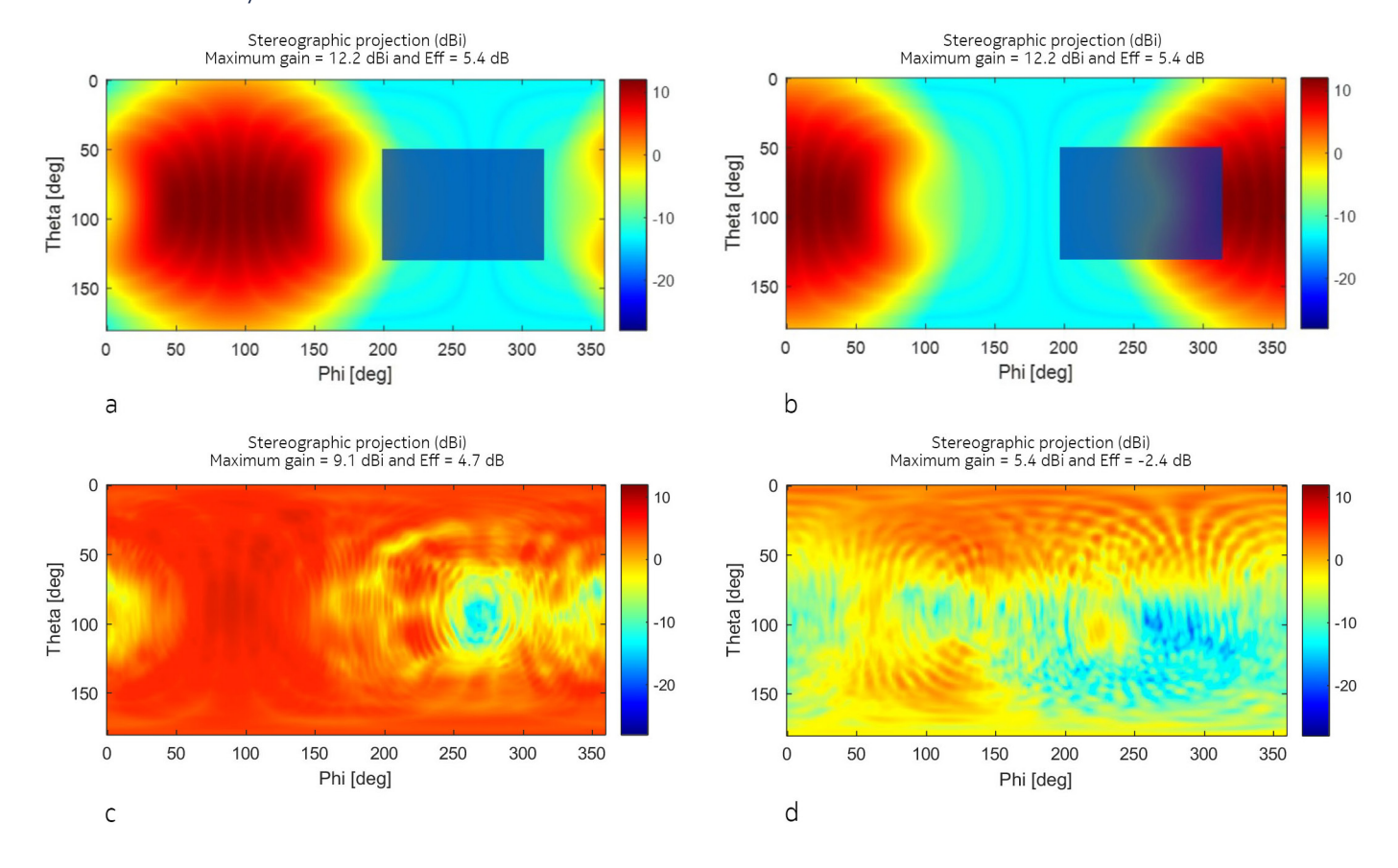
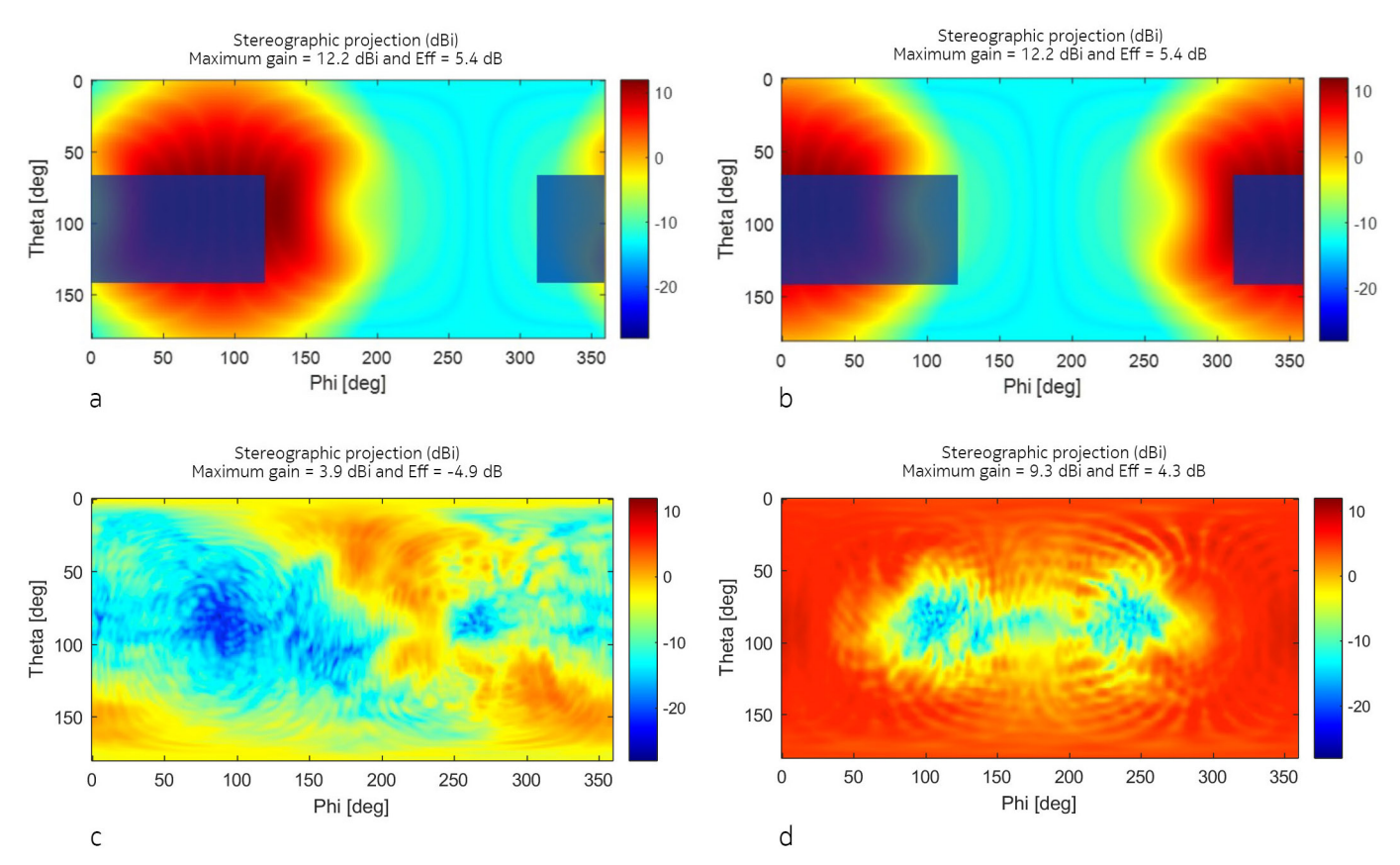




Figure 23: 3GPP blockage model for dual-hand browsing grip: a) 3GPP model for antenna array 1; b) 3GPP model for antenna array 2; c) Simulated results for antenna array; and d) Simulated results for antenna array 2.



The angular power distribution for the 3GPP antenna model including blockage is very different to the CST simulated result, including hand phantoms. The question is how big an impact these observed differences will have on LLS and SLS simulation results.

This has partly been investigated in the [Institute of Electrical and Electronics Engineers (IEEE) published Access paper], where the following results are derived via LLS, using different blockage scenarios.



Table 11: Received signal strength at different percentiles obtained through LLS simulations

Blockage scenario	Received signal str	Received signal strength [dBm]					
	10th	50th	90th				
3GPP FS portrait	-98.6	-72.3	-51.5				
3GPP one-hand blockage	-110.7	-73.7	-52.3				
3GPP FS landscape	-99.7	-72.0	-52.0				
3GPP dual-hand blockage	-110.4	-77.2	-55.5				
CST FS portrait	-97.1	-73.2	-52.9				
CST RHB grip	-101.0	-75.5	-55.4				
CST FS landscape	-97.1	-73.2	-53.2				
CST DHB grip	-101.0	-76.2	-55.5				
CST GHB grip	-102.0	-78.1	-55.8				

Table 12 shows the differences between the 3GPP models and the CST simulated models (i.e., RHB, DHB, DHG) when evaluated on Received Signal Strength Indicator (RSSI) by LLS, including UE mobility and rotation.

Table 12: Delta received signal strength for different blockage scenarios

Blockage scenario	Delta received signal strength [dB]				
	10th	50th	90th		
Delta values FS portrait	-1.5	0.9	1.4		
Delta values FS landscape	-2.6	1.2	1.8		
Delta values one-hand browsing (RHB)	-9.7	1.8	3.1		
Delta values dual-hand browsing (DHB)	-9.4	-1.0	0.0		
Delta values dual-hand browsing (DHG)	-8.4	0.9	0.3		

This LLS investigation shows that the 3GPP models tend to overestimate the worst-case scenarios (10th percentiles) by up to 10 dB and the best-case scenarios (90th percentiles) by up to 3 dB, when compared to the results obtained with CST simulations, including hand phantoms.

Conclusion from the paper:

Finally, results suggest that the current blockage model proposed by 3GPP must be further enhanced to account for blockage on a per-panel basis. This would allow a more accurate portrayal of user hand behavior, which would support the analysis and design of effective solutions to overcome the user's unpredictable shadowing effects at mmWave frequencies.



User interaction comparison with FR1 implementation

The antenna performance at FR1 has been simulated on a similar reference smart phone design, as shown in Figure 3 for FR2. The TRE values are shown in Table 13 for the required two LB antennas at 800 MHz and the four HB/MB/UHB antennas at 1900 MHz, where it can be seen that the loss introduced by the user's hand can be significantly higher than that observed for FR2 (see Table 9).

Table 13: Examples of simulated TRE for different FR1 antennas and different use cases

	Total radiation effi	Total radiation efficiency				
Antenna	Frequency	Free space	Talk position	Delta		
Ant#1	800 MHz	-6.5 dB	-14.0 dB	-7.5 dB		
Ant#2	800 MHz	-6.5 dB	-22.9 dB	-16.4 dB		
Ant#3	1900 MHz	-5.1 dB	-13.2 dB	-8.1 dB		
Ant#4	1900 MHz	-5.1 dB	-9.9 dB	-4.8 dB		
Ant#5	1900 MHz	-5.1 dB	-13.3 dB	-8.2 dB		
Ant#6	1900 MHz	-5.1 dB	-29.7 dB	-24.6 dB		

The results in Table 13 are based on simulated antenna gain values, so they only include the absorption loss and not the loss contributed from the antenna matching and frequency tuning circuits. Antennas at FR1 frequencies are impedance bandwidth limited, due to the small volume allocated for the antenna design in the form factor of modern smart phones. Because of this, it is necessary to include frequency tuning of the antennas to match them to the active 5G NR bands, whereby an antenna operating at FR1 will typically only be capable of supporting one 5G NR band at any given time.

Only two different frequencies (800 MHz and 1900 MHz) are evaluated for the FR1 reference smart phone form factor, as the performance at adjacent frequencies will be similar when performing the evaluation based on simulated antenna gain values.

XR antenna implementation for 5G NR

Extended Reality (XR) is a 3GPP definition covering the following three types of realities:

- Augmented Reality (AR): adding virtual objects to real-world environments.
 - Devices: tablets and glasses.
- Virtual Reality (VR): visual and audio scene combined with real-world locations.
 - Devices: usually Head Mounted Displays (HMDs).
- Mixed Reality (MR): adding haptics and interactions.
 - Devices: glasses, controllers.

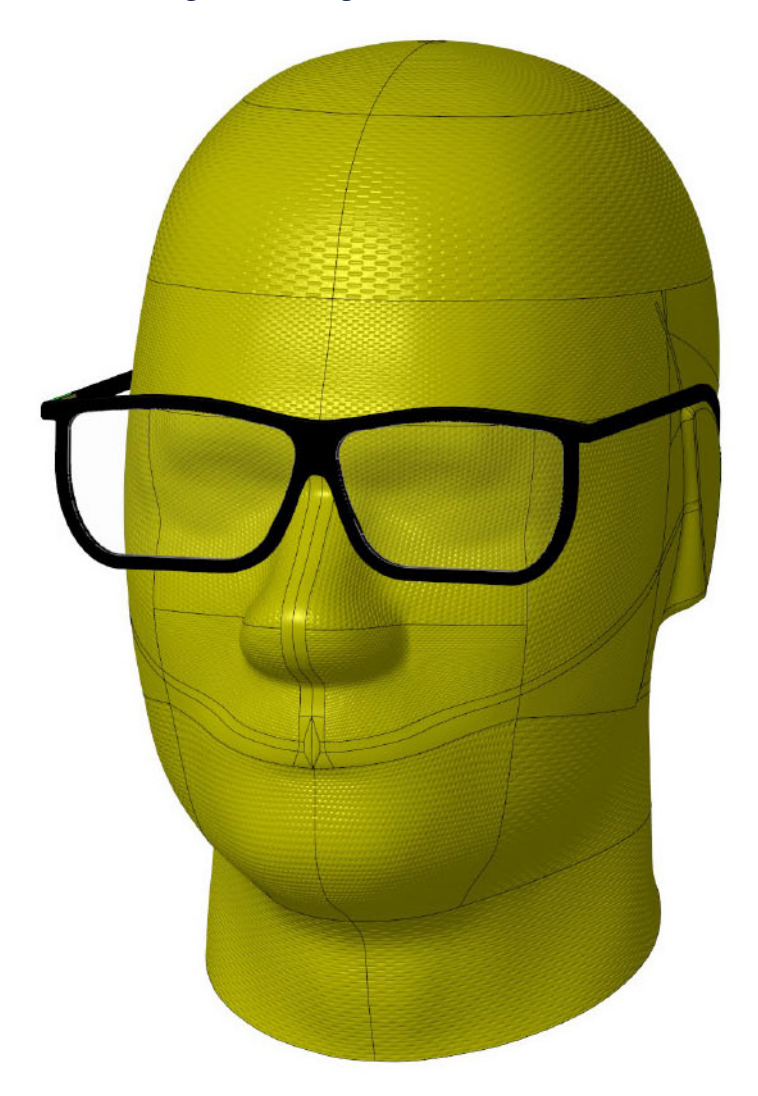
In general, XR will require high data rates for high-resolution images, with a high refresh rate and low latency. Using the mmWave system bands is an obvious solution due to the wide available bandwidth per carrier (400 MHz) for high throughput, and the short symbol duration time (8.33 µs) for low latency.



However, this could be a design challenge for certain types of XR devices, as discussed below.

The focus of this evaluation is on glasses and their expected performance at mmWave frequencies, more specifically at 28 GHz. As shown in Figure 24, the glasses feature a slim design, as a bulky industrial design would not be appealing to consumers for aesthetic reasons. In addition, the design of the reference glasses is optimized to fit the Specific Anthropomorphic Mannequin (SAM) head phantom defined by IEEE and adopted by CTIA.





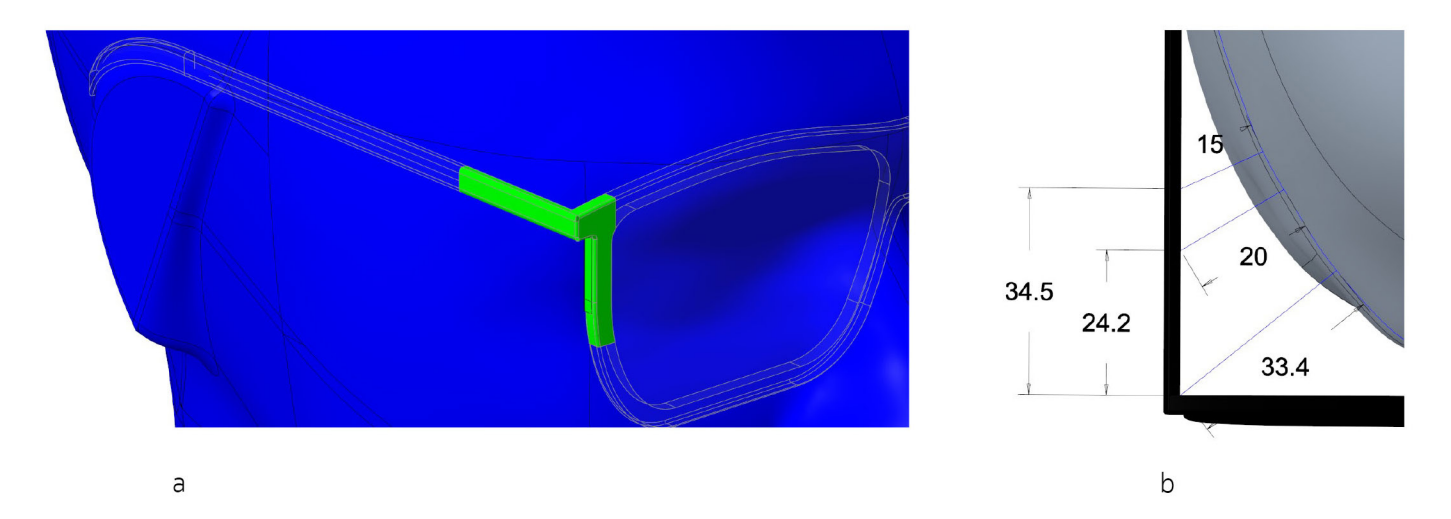
Two different 1x4 antenna array implementations are considered on the slim Nokia reference glasses.

- The expected/intuitive implementation in the temple of the glasses: A horizontally aligned 1x4 antenna array with dual polarized patch elements (two isolated orthogonal patch feed points that can be used simultaneously with two different signals).
- Alternative implementation in the frame/rim of the lenses: A vertically aligned 1x4 antenna array with single polarized monopole elements (only one element feed point, so only a single signal can be utilized at any given time).



The optimal placement of a 1x4 antenna array implementation is illustrated in Figure 25 (part a) by the highlighted green color on the frame of the glasses. This placement is optimal as it ensures maximum distance between the implemented antenna arrays and the SAM head phantom, as illustrated in Figure 25 (part b). This will lead to better efficiency and reduced electromagnetic exposure to the user's head. The Maximum Permissible Exposure (MPE) is regulated by the [Federal Communications Commission (FCC)] with a maximum Power Density (PD) level of 1W/m2 or 1mW/cm2. This evaluation is the average value for an area of 4 cm2 (2 cm x 2 cm).

Figure 25: Optimal placement of an antenna array on a pair of XR glasses: a) the optimal placement; and b) Direct distances between the reference XR glasses and the SAM phantom.



3GPP requirements

3GPP has so far defined four different power classes for user equipment, which are defined as follows:

- Power Class 1: Fixed Wireless Access (FWA) UE
- Power Class 2: Vehicular UE
- Power Class 3: Handheld UE
- Power Class 4: High power non-handheld UE

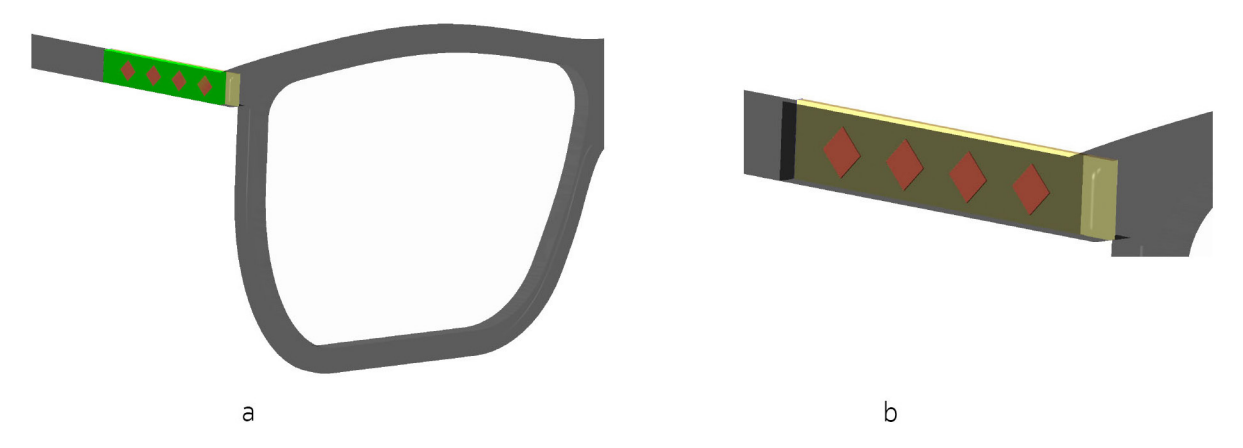
Power class 3 is the best suited class for XR glasses, as it is currently defined in the 3GPP specifications and is used for the performance evaluation described in section 3.2 (see section 1.3 for a short summary of the specific 3GPP requirements). However, a new power class for XR devices, including certain types of low-power, short-range XR devices, may be defined later within 3GPP if needed.



Envisioned implementation on a pair of glasses and expected performance

An intuitive approach is to implement a 1x4 antenna array into each of the temples, as illustrated in Figure 26 for the right temple. The alignment of the dual polarized patch elements is in diamond orientation to ensure similar performance of both isolated orthogonal polarization excitations, as they are symmetrically placed with respect to other array patch elements and the array ground plane. The size of the antenna array is $1.00 \times 27.50 \times 1.75$ mm (W x L x T). An advantage of this implementation is that each antenna array can support 2x2 MiMo, and an implementation with two antenna arrays is capable of supporting 4x4 MiMo. However, this implementation will require traditional beam steering, as shown in Figure 26.

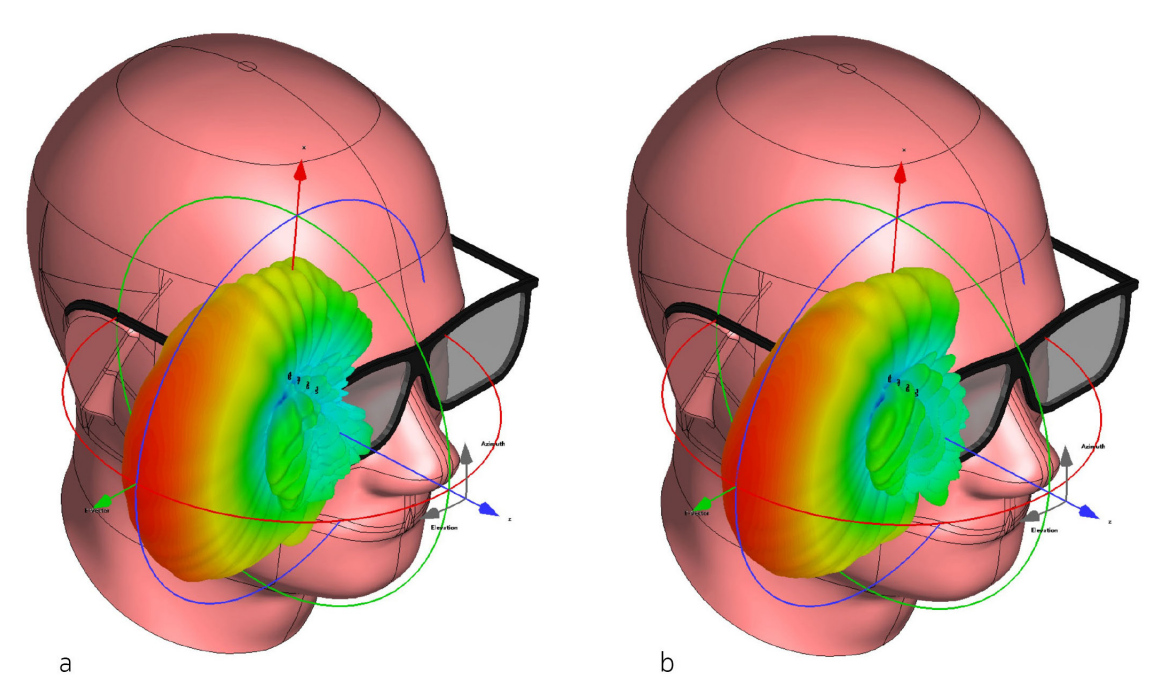
Figure 26: Intuitive Implementation of a 1x4 antenna array in the right temple: a) Placement in the right temple; and b) The antenna array design.



The simulated boresight radiation patterns for this intuitive implementation are shown Figure 27 for the Co-Polarized (Co-Pol) and Cross-Polarized (Cross-Pol) feedings of the antennas array. The difference between two boresight radiation patterns is insignificant as the individual patch elements have a diamond orientation compared to the ground plane.

NOSIA

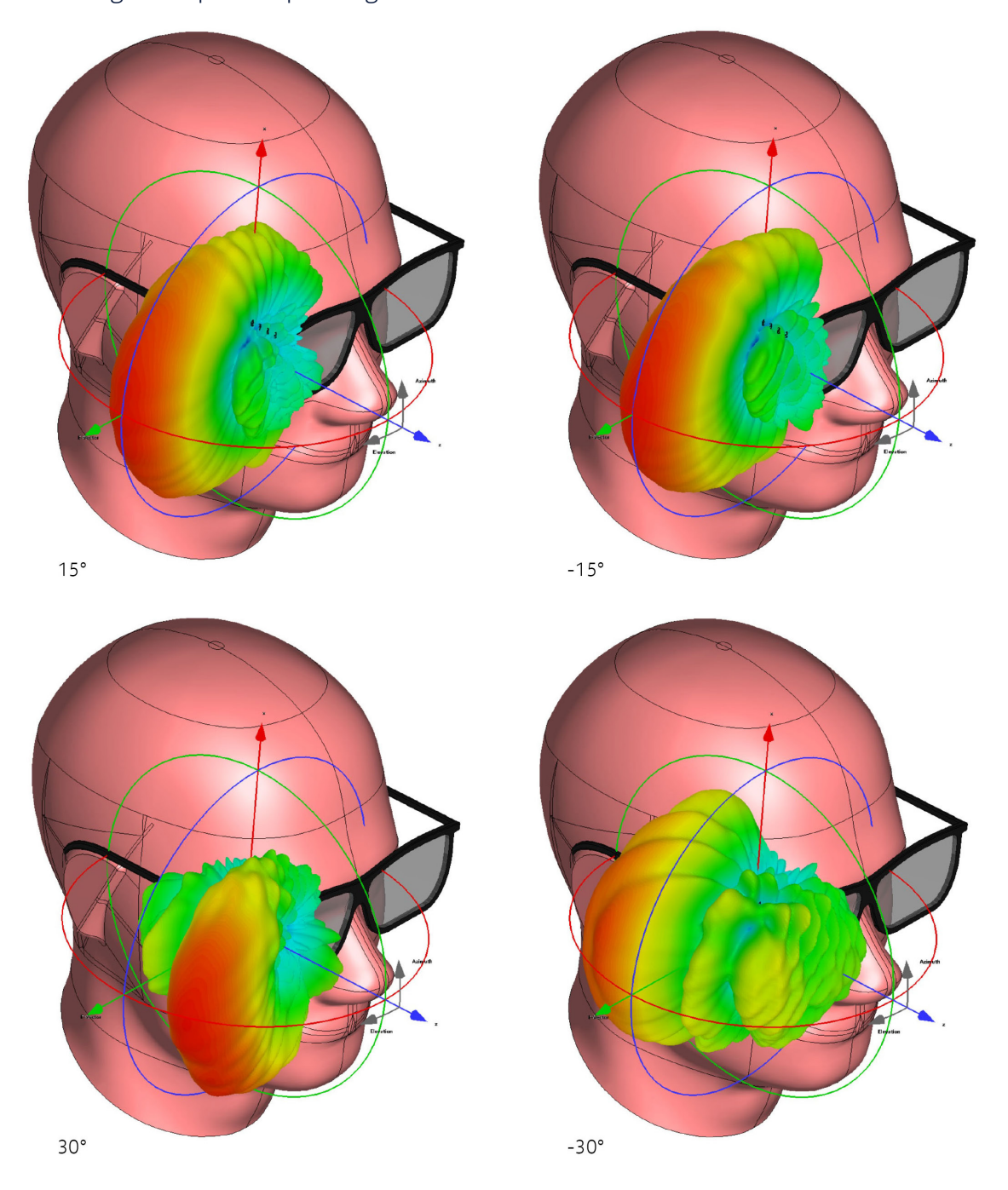
Figure 27: Boresight radiation patterns for the Co-Pol (a) and Cross-Pol (b) feedings.



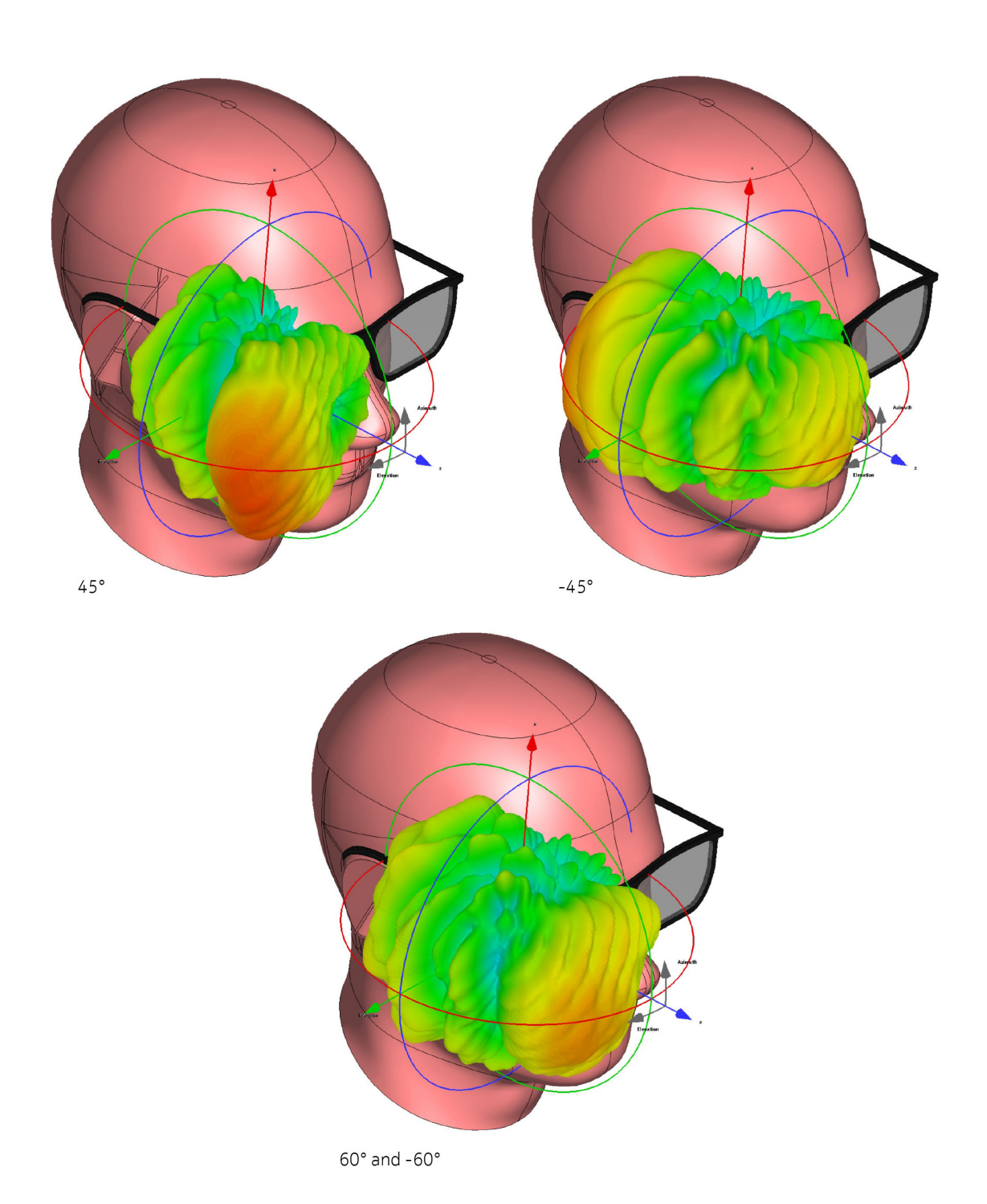
The proposed beam steering configurations for this implementation are shown in Figure 28 for 8 additional beams (-60°, -45°, -30°, -15°, 15°, 30°, 45°, and 60°) and Co-Pol feedings. The 60° beams configurations are included for the glasses to obtain better spherical coverage, as this example will only include two antenna arrays, which are mirrored versions of each other implemented in the right and left temple.



Figure 28: Envisioned beam configuration for a 1x4 antenna array operating at 28 GHz and implemented in the right temple of a pair of glasses



NOKIA

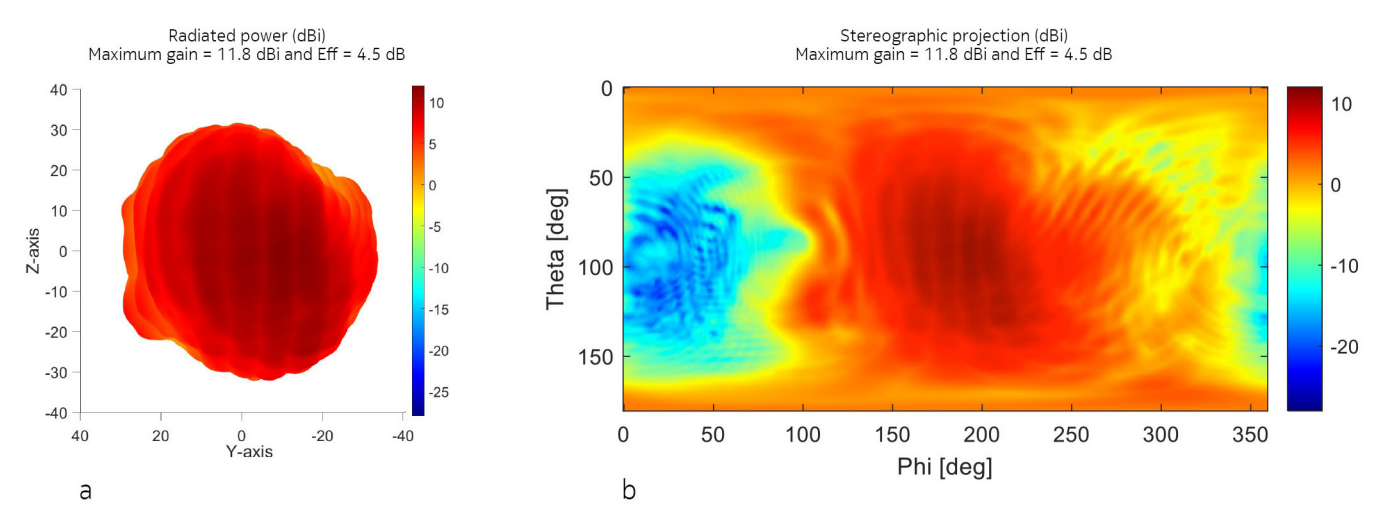


٠



Figure 29 shows the antenna gain power envelope of all the eight individual beam configurations (shown in Figure 28) as a 3D plot and a stereographical projection.

Figure 29: Antenna gain power envelope of all individual beam configurations: a) 3D plot; and b) Stereographical projection.



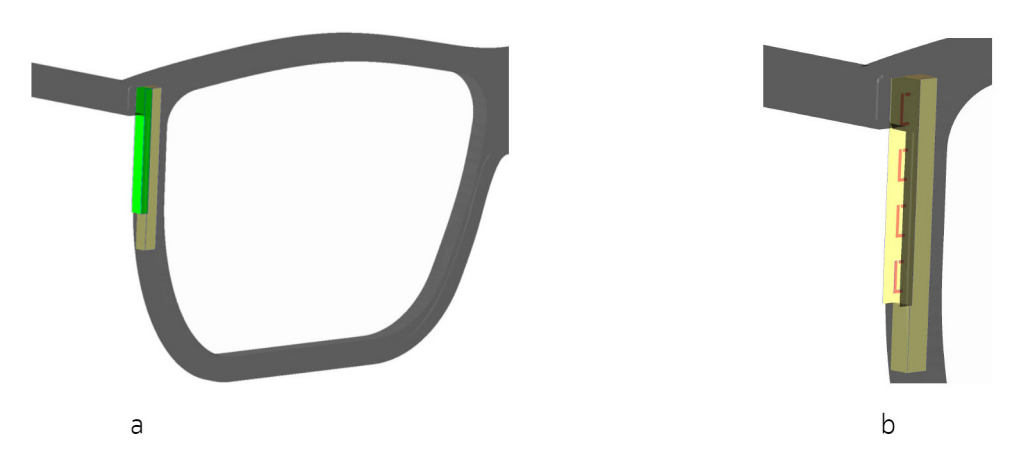
The simulated maximum antenna gain value (11.8 dBi) is similar to the maximum antenna gain obtained for a standalone 1x4 antenna array at 11.9 dBi, as shown in Figure 20 (parts b and e). This indicates that this horizontal placement of the antenna array is optimal as it behaves as it does in free space, due to a maximized distance to the head of the user, as illustrated in Figure 25.



Alternative implementation on a pair of glasses and expected performance

An alternative implementation is to implement the antenna array in the vertical part of the frame of the lenses, as illustrated for the right lens in Figure 30.

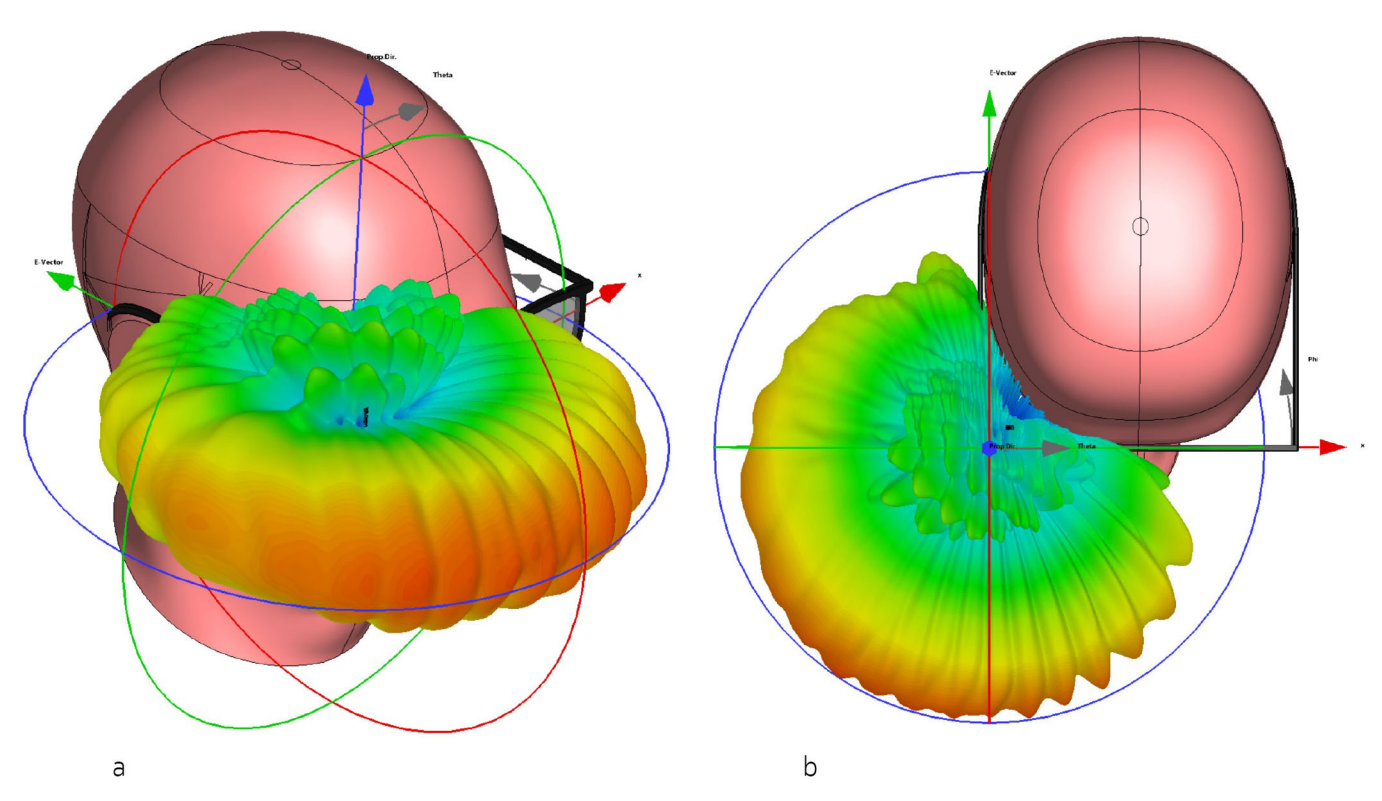
Figure 30: Alternative implementation of a mmWave antenna array on a pair of XR glasses: a) Placement of the frame/rim of the lenses; and b) Antenna array design.



This implementation only allows an antenna array using single monopole elements, due to the reduced space for the antenna array with this slim reference XR glass design. As a result, each array can only support a single data stream and will require an additional antenna array at the left frame/rim of the lens for 2x2 MiMo operation. However, an advantage of this implementation is that it will not require beam steering, as the antenna gain of the radiation pattern is orientated in the horizontal plane, as shown in Figure 31.

NOSIA

Figure 31: Horizontal radiation pattern for the alternative implementation of a 1x4 antenna array: a) Perspective view; and b) Top view.



The user's head, and therefore the XR glasses, will be in an upright position for most use cases, because the user will typically be either walking or sitting. This is a semi-static environment where the horizontal dimension is more or less fixed. As a result, the horizontal radiation pattern achieved with this alternative implementation will be the optimal choice for most use cases because beam steering will not be needed. This can reduce the complexity of the antenna array Radio Frequency (RF) design and reduce the implementation loss by a few dBs, as the insertion loss of a phase shifter, which is required for analog beam steering, can be quite high (typically 5 dB) depending on the granularity.

One situation where such a static high-gain beam configuration might not be optimal occurs when the user is close to a high, elevated gNB (typically around 30 meters), where the power will arrive from a higher elevation angle. However, this can be detected and solved by reducing the number of activated elements on the antenna array. This is illustrated in Figure 32, where only 2 or 1 elements are activated.

NOSIA

Figure 32: Radiation patterns when activating a reduced number of elements: a) 2 elements activated; and b) 1 element activated.

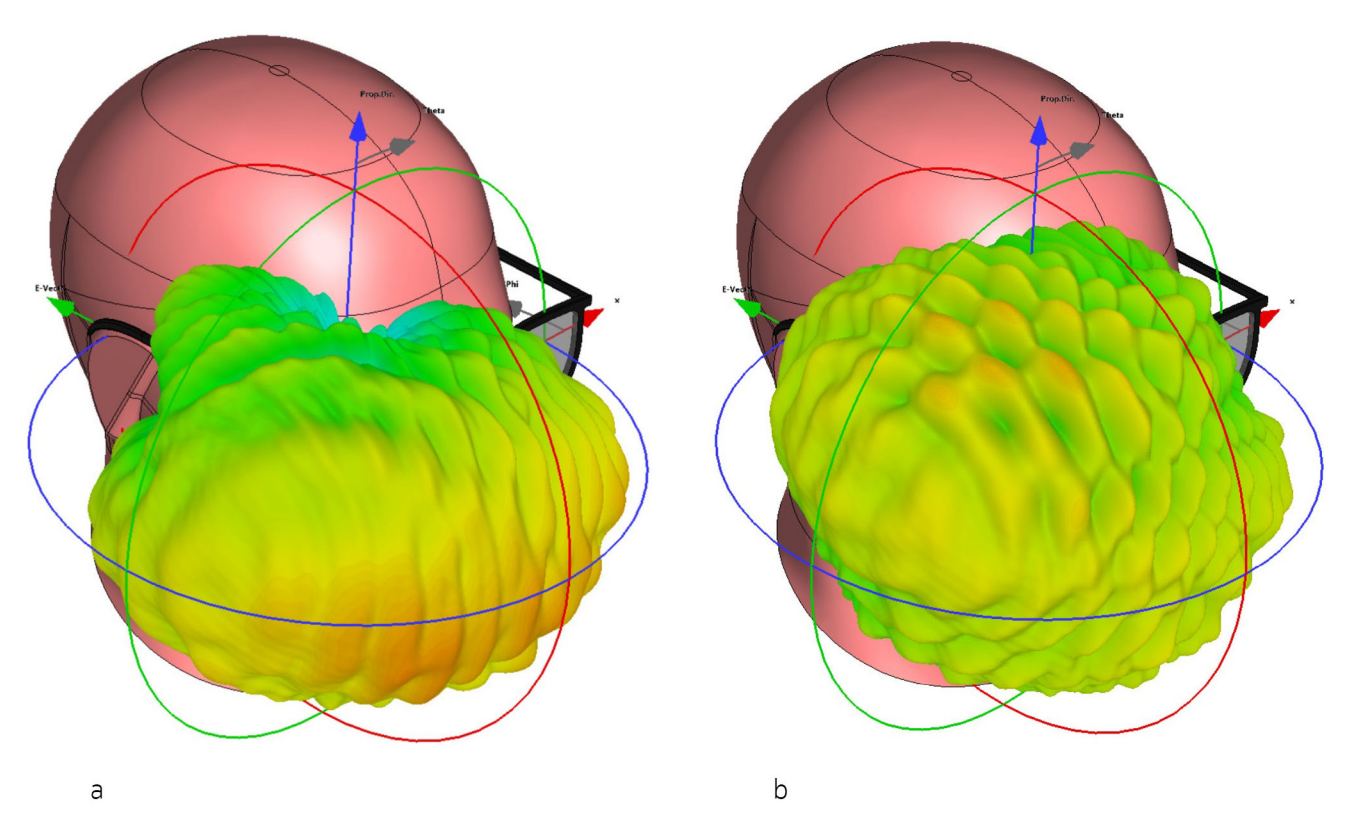
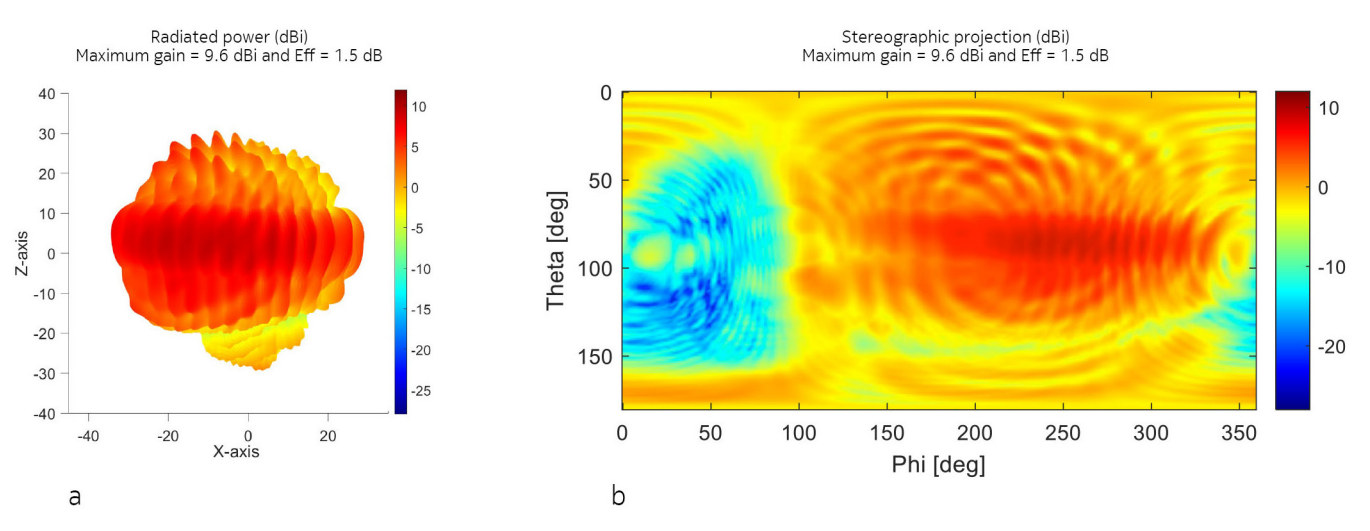


Figure 33 shows the antenna gain power envelope of all the eight individual beam configurations (shown in Figure 31 and Figure 32) as a 3D plot and a stereographical projection.

Figure 33: Antenna gain power envelope of all individual beam configurations: a) 3D plot; and b) Stereographical projection.





The simulated antenna gain values for the three different antenna array element activation configurations are shown in Table 14.

Table 14: Simulated antenna gain values for different numbers of activated elements

Simulated antenna gain				
4 elements	2 elements	Single element		
9.6 dBi	7.5 dBi	6.1 dBi		

The obtained maximum antenna gain value when all four elements are activated is less than that obtained for a standalone 1x4 antenna array (9.6 dBi vs. 11.9 dBi). This is not due to reduced antenna efficiency, but due to the electrical properties of the lenses that are right next to this alternative implementation of the antenna array. The lenses act as waveguides and are spreading the radiated energy in more angular directions, thereby also reducing the maximum achievable antenna gain.

Estimated performance for an mmWave antenna array on a pair of XR reference glasses

The maximum EIRP for a boresight configuration can be derived from the simulated maximum antenna gain values shown in Table 14, using the following assumptions:

- Power delivered to the antenna array is 23 dBm from the PA.
- An implementation loss of 8 dB is added to represent a realistic antenna array design integrated into a pair of slim XR glasses.

The implementation loss used is 2 dB higher than what is used for the smart phone form factor, because the mechanical implementation of the antenna array is more complex for this use case, and the volume available for the antenna array is smaller.

The maximum Peak EIRP values for the two implementations are estimated to be the following:

- 26.8 dBm for the intuitive implementation
- 24.6 dBm for the alternative implementation

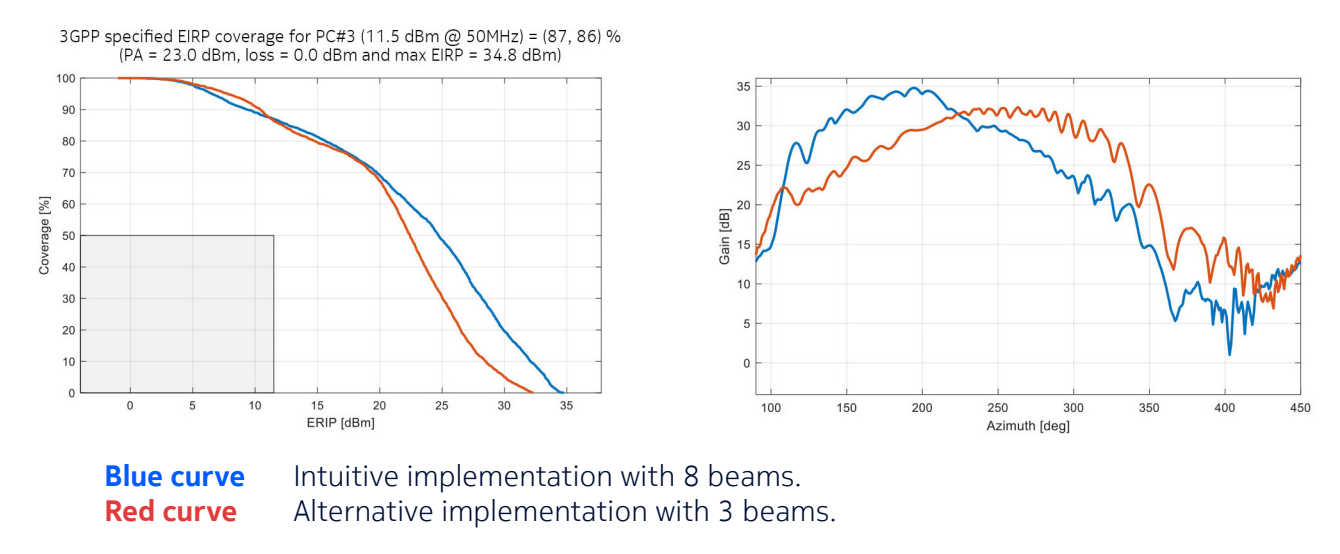
Both implementations are compliant with the required minimum peak EIRP of 22.4 dBm as specified by 3GPP for a PC3 UE (see Table 1).

The spherical EIRP coverage for the power envelope of the intuitive implementation, including eight beam configurations, and for the alternative implementation, including three beam configurations, is shown in Figure 34 (part a). The 3GPP spherical requirement (see Table 1) for EIRP PC3 is illustrated with the gray box in the plots; however, the specification for XR devices has not yet been defined, so this could be modified.

White paper

NOKIA

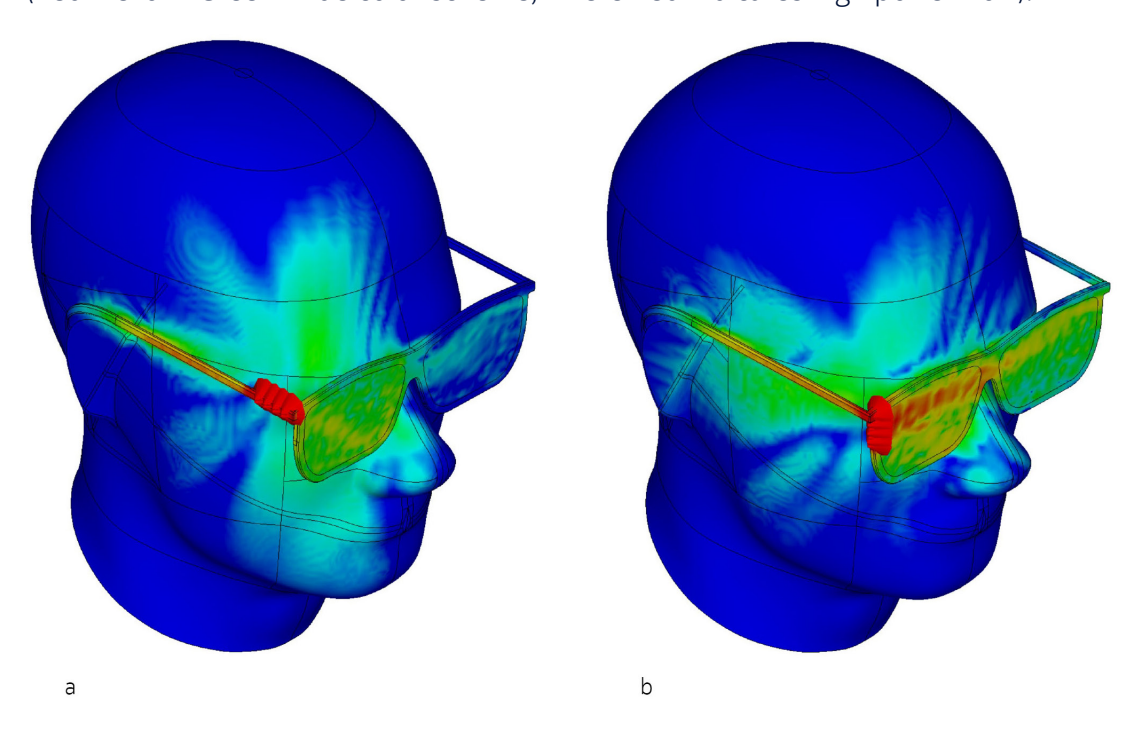
Figure 34: a) Spherical EIRP coverage CCDF curves; and b) Top view 2D plot of the power envelope.



The spherical EIRP coverage is similar at 11.5 dBm (87% vs 86 %, as shown in the figure text), but the intuitive implementation has higher maximum EIRP values and better coverage for the lower half percentiles (<60 % @ 20 dBm EIRP). However, this is obtained by using more configurable beams (8 vs. 3).

An MPE evaluation has been made for both antenna array implementations, and the power flow for each is shown in Figure 35 for boresight beam configurations.

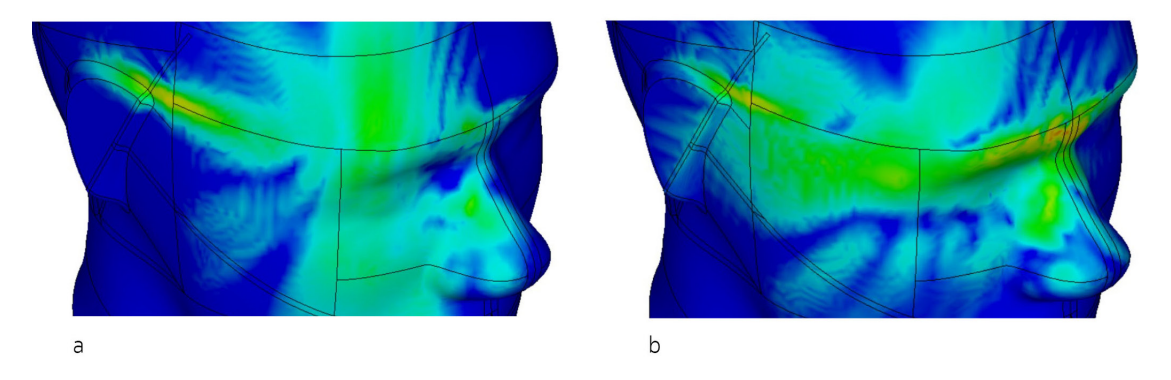
Figure 35: Power flow for each antenna array implementation: a) Intuitive; and b) Alternative (Red>Yellow>Green>Blue color scheme, where Red indicates high power flow).





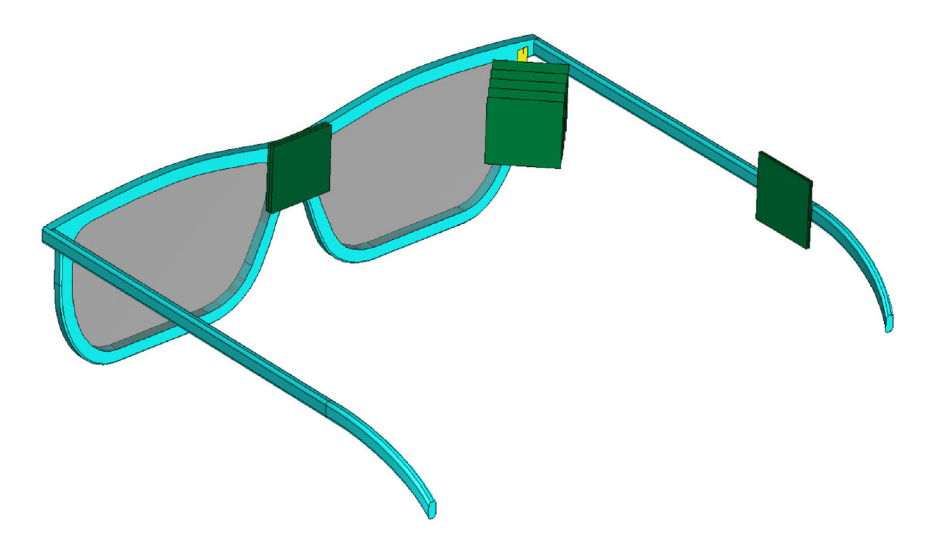
The data shows that the alternative antenna array implementation couples more power into the lenses of the glasses, as mentioned above, whereas the power flow on the SAM phantom seems to be at the same level. The high PD regions on the SAM phantom (see Figure 35) are located in the eyebrow/nose area where the nose supports the glasses; the ear area supporting the temple; and the area on the phantom closest to the antenna array, the direct coupling.

Figure 36: Power flow on the SAM phantom alone: a) Intuitive; and b) Alternative (Red>Yellow>Green>Blue color scheme where Red indicates high power flow).



The MPE is evaluated in FS on different 2 cm x 2 cm surfaces around the areas mentioned above, as shown in Figure 37.

Figure 37: Surfaces areas (2 cm x 2 cm) used for MPE evaluation



The MPE evaluation areas are located with the following distances towards the SAM phantom:

- Eyebrow/nose area > 0.25, 1.25 and 2.25 mm
- Antenna array area > 10, 15, 20, 25 and 30 mm
- Ear area > 0.25, 0.75 and 1.25 mm



The MPE evaluation results are summarized in Table 15, for 23 dBm power delivered to the antenna array and full duty-cycle.

Table 15: Simulated MPE values and maximum allowed PA power

	Intuitive implementation		Alternative implementation	
	PD @ 23 dBm PA power [mW/cm²]	Max PA allowed power [dBm]	PD @ 23 dBm PA power [mW/cm²]	Max PA allowed power [dBm]
At Eyebrow/Nose	0.1	34.3	2.0	20.0
At Ear	1.3	21.7	0.9	23.6
Direct distance	0.2	29.4	0.4	26.6

Table 15 shows that the MPE values for a 100% Tx duty-cycle are generally below the limit dictated by FCC at a maximum 1.0 mW/cm2. However, the intuitive implementation is above the limit for the area near the ear, while the alternative implementation is above the limit for the area near the eyebrow/nose. The maximum Tx duty-cycle with the current 3GPP release 17 is 20%, so the maximum allowed PA power values in Table 15 can be increased by a factor of 5 or approximately 7 dB, whereby all values will be higher than 23 dBm and will not require power back-off due to MPE.

Note that this conclusion is based on the current FCC requirements for handheld devices, which may not comply with a pair of glasses.

Alternative mmWave antenna solution

MmWave communications, as introduced for 5G NR, enable new types of antennas for devices supporting these new FR2 bands. The type of antenna implemented depends on the expected range between the gNB and the device, where increased antenna aperture at the devices is required for inter-cell-site distances of several hundreds of meters. This is the reason 3GPP assumes that most devices supporting mmWave are implemented with one or more antenna arrays (in most cases 1x4 antenna arrays), where the performance has been estimated and evaluated against the requirements derived by 3GPP.

One of the biggest implementation challenges of this antenna array concept involves finding the space in the devices to implement the 1x4 antenna arrays, while at the same time achieving a high level of radiation efficiency in the antenna array. This is especially challenging for smart phone implementations, as the aesthetics of the industrial design of these devices are very important and the allocated space and volume available for the mmWave antenna array is limited, due to a compact mechanical build. As such, an antenna array at the side edge of a smart phone will have to be slim (low height) to maximize the volume available for the battery, and an antenna array at the front or rear of the phone will also have to be slim to maintain the low height of the phone. A low profile/height antenna array will have an increased Q-factor for each element, which will decrease the impedance bandwidth and increase the field strength of the H- and E-fields, which will in turn increase the absorption loss and reduce the radiation efficiency. The routing from the RF module containing the PAs and Low Noise Amplifiers (LNAs) to the individual elements in the antenna array will in itself increase the loss, in addition to the loss added from the required phase shifters for beam steering.



A 1x4 antenna array will in theory add 6 dB of antenna gain in the direction of the main beam lobe, compared to a single element. However, this is only true if the radiation efficiency of the individual elements in the antenna array is equal to the radiation efficiency of the stand-alone element. This is the real challenge for mmWave antenna implementation in devices where the industrial design is more important than antenna performance. Stand-alone monopole antennas can be implemented more easily in a smart phone, wherever a small amount of space is available. This can be achieved with a radiation efficiency of -3 dB, for example. The typical radiation efficiency of mmWave antenna arrays in the industry is around -8 dB, which is much lower than what should be achievable for a stand-alone monopole. Assuming a maximum delivered power to the antenna of 23 dBm and an antenna gain of 6 dB for the individual elements in the antenna array, and for the stand-alone monopole antenna, then the antenna array will have a maximum EIRP of 27 dBm, where the stand-alone monopole antenna will have a maximum EIRP of 26 dBm.

1x4 antenna array

Power to the antenna + element gain + array gain + radiation efficiency = 23 dBm + 6 dB + 6 dB - 8 dB = 27 dBm.

Monopole antenna

Power to the antenna + element gain + radiation efficiency = 23 dBm + 6 dB - 3 dB = 26 dBm.

As a result, both implementations will have a similar maximum EIRP, as well as a similar link level performance. This issue is not seen within 3GPP LLS and SLS, as the efficiency of antenna elements is the same, with no consideration given to implementation losses for different kinds of devices or to the increasing size of the antenna arrays.

Are antenna arrays always the best choice of antenna type for all supported 3GPP devices where the industrial design has higher priority than the antenna performance (e.g., for smart phones, XR glasses and smart watches)? It's important to note that the stand-alone monopole antenna implementation is cheaper, less complex, and less intrusive to the industrial design. Antenna array designs for other devices like Customer Premises Equipment (CPE), Ambient Internet of Things (A-IoT), Network Controlled Repeater (NCR), and vehicular devices might still be the best choice, as the antenna performance can be optimized for such devices.



Conclusion

The introduction of mmWave frequencies within 5G NR has also introduced new types of antenna solutions for the devices supporting these frequencies. The initial solution envisioned by 3GPP and the solution adopted by the industry is multiple 1x4 antenna arrays (2 to 3) for smart phone form factors. However, these implementations are lossy and some of the commercial devices on the market today have a maximum peak EIRP just above the required level of 22.4 dBm minimum peak EIRP for system bands within the 28 GHz frequency range. Some of the high-end devices have maximum peak EIRPs that are 2 to 4 dB higher than the requirements, but that still indicates an antenna implementation with absorption losses in the range of 8 dB, assuming a delivered PA power to the antenna array of 23 dBm. The larger antenna aperture in the form of antenna arrays needed for improved system performance is difficult to implement without introducing high absorption losses, which are mostly due to the reprioritization of antenna performance to achieve appealing industrial design.

The current 3GPP requirements for minimum peak EIRP and coverage are very lenient. These requirements will in theory allow devices with antenna implementation/absorption losses as high as 12 dB for a 1x4 antenna array, with a delivered PA power of 23 dBm. Or they may even allow simple monopole designs with no increased antenna aperture. As such, the improved antenna array gain from the increased antenna aperture envisioned for increased coverage, is typically lost due to a very high implementation loss, which is allowed with the current 3GPP radiated requirements.

A simple solution to improve device performance involves introducing a new power class with increased minimum peak EIRP for mmWave system bands within 3GPP. This would result in better mmWave performance in terms of network efficiency, throughput and coverage and give the user a better experience. A better solution would be to increase the minimum peak EIRP power level for the current PC3, as that would increase the performance for all devices supporting mmWave system bands.

The performance of XR devices like glasses are still in the definition phase within 3GPP and different modes of connectivity are being discussed. One mode involves tethering to a nearby smartphone (onbody network) and a second mode involves direct connection to the network. Both FR1 and FR2 frequency ranges are still in play depending on the application, the required data rate and latency. Direct connectivity to the network at mmWave frequencies is in theory possible, as highlighted by the simulations presented in this whitepaper, with two implementations with different complexity and design challenges. However, the determining factor will be the implementation/absorption loss, which will likely be dictated by the priority of the industrial design. This would enable devices for industrial applications, where performance is more important than aesthetics, to connect directly to the network, while consumer devices might rely on the on-body network, utilizing a smart phone as a network connection, given how important aesthetics are for these types of devices.



Abbreviations		IEEE:	Institute of Electrical and Electronics Engineers
3GPP:	3rd Generation Partnership Project	LB:	Low-band
5G:	Fifth Generation NR	LLS:	Link Level Simulations
A-IoT:	Ambient Internet of Things	MB:	Mid-band
AMPS:	American Mobile Phone System	MIB:	Master Information Block
AR:	Augmented Reality	MiMo:	Multiple Input Multiple Output
CA:	Carrier Aggregation	MLB:	Mid-low-band
CCDF:	Complementary Cumulative Distribution Function	MPE:	Maximum Permissible Exposure
CDF:	Cumulative Distribution Function	MR:	Mixed Reality
Co-Pol:	Co-Polarized	NCR:	Network Controlled Repeater
CPE:	Customer Premises Equipment	NMT:	Nordic Mobile Telephone
CQI:	Channel Quality Indicator	NR:	New Radio Access
Cross-Pol:	Cross-Polarized	OTA:	Over the Air
CSI:	Channel State Information	PA: PC3:	Power Amplifier Power Class 3
CSI-RS:	Channel State Information Reference	PC3. PD:	Power Density
Signal		RACH:	Random Access CHannel
CST:	Computer Simulation Technology	RF:	Radio Frequency
CTIA:	TIA: Cellular Telecommunications Industry Association		Right Hand Browse
DHB:	Dual Hand Browse	RI:	Rank Indicator
DHG:	Dual Hand Gamer	RO:	RACH Opportunity
DL:	Downlink	RS:	Reference Signal
EIRP:	Equivalent Isotropic Radiated Power	RSRP:	Reference Signal Received Power
EIS:	Equivalent Isotropic Sensitivity	RSSI:	Received Signal Strength Indicator
FCC:	Federal Communications Commission	Rx:	Receive
FR1:	Frequency Range 1	SAM:	Specific Anthropomorphic Mannequin
FR2:	Frequency Range 2	SIB1:	System Information Block 1
FS:	Free Space	SLS:	System Level Simulations
FWA:	Fixed Wireless Access	SMS:	Short Message Service
gNB:	NR Base Station	SNR:	Signal to Noise Ratio
HB:	High-Band	SSB:	Synchronization Signal Block
IE:	Information Element	TR:	Technical Report



TRE: Total Radiated Efficiency UE: **User Equipment** TRP: **Total Radiated Power** UHB: Ultra-High-Band Virtual Reality TS: **Technical Specifications** VR: Tx: **Transmit** XR: **Extended Reality**

References

[3GPP TR 38.802 section 6.1.6]

https://portal.3gpp.org/desktopmodules/Specifications/SpecificationDetails.aspx?specificationId=3066

[TS 38.214 section 5.2]

https://portal.3gpp.org/desktopmodules/Specifications/SpecificationDetails.aspx?specificationId=3216

[TS 38.101-2]

https://portal.3gpp.org/desktopmodules/Specifications/SpecificationDetails.aspx?specificationId=3284

[CST Microwave Suite®]

https://www.3ds.com/products-services/simulia/products/cst-studio-suite/

[CTIA]

https://ctiacertification.org/program/over-the-air-performance-testing/

[3GPP, TR 38.803, Table 5.2.3.3]

https://portal.3gpp.org/desktopmodules/Specifications/SpecificationDetails.aspx?specificationId=3069

[Institute of Electrical and Electronics Engineers (IEEE) published Access paper]

Fernandes, Filipa: Hand Blockage Impact on 5G mmWave Beam Management Performance https://ieeexplore.ieee.org/stamp/stamp.jsp?arnumber=9908554

[Federal Communications Commission (FCC)] FCC: Evaluating Compliance with FCC Guidelines for Human Exposure to Radiofrequency Electromagnetic Fields (https://transition.fcc.gov/oet/info/documents/bulletins/oet65/oet65a.pdf)

About Nokia

At Nokia, we create technology that helps the world act together.

As a B2B technology innovation leader, we are pioneering networks that sense, think and act by leveraging our work across mobile, fixed and cloud networks. In addition, we create value with intellectual property and long-term research, led by the award-winning Nokia Bell Labs.

Service providers, enterprises and partners worldwide trust Nokia to deliver secure, reliable and sustainable networks today – and work with us to create the digital services and applications of the future.

Nokia is a registered trademark of Nokia Corporation. Other product and company names mentioned herein may be trademarks or trade names of their respective owners.

© 2023 Nokia

Nokia OYJ Karakaari 7 02610 Espoo Finland Tel. +358 (0) 10 44 88 000 629906 (August) CID213454